

D- π -A Compounds with Tunable Intramolecular Charge Transfer Achieved by Incorporation of Butenolide Nitriles as Acceptor Moieties

Carlos Moreno-Yruela,[†] Javier Garín,[†] Jesús Orduna,[†] Santiago Franco,[†] Estefanía Quintero,[‡] Juan T. López Navarrete,[‡] Beatriz E. Diosdado,[§] Belén Villacampa,^{||} Juan Casado,^{*,‡} and Raquel Andreu^{*,†}

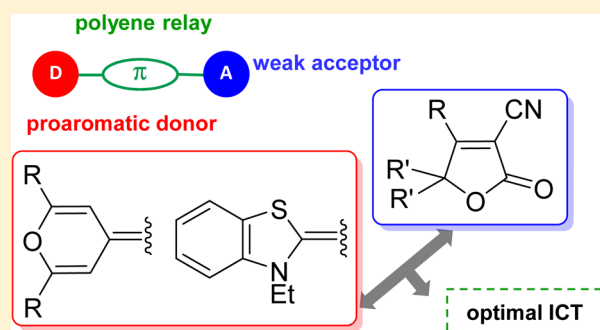
[†]Departamento de Química Orgánica, ICMA, and ^{||}Departamento de Física de la Materia Condensada, ICMA, Universidad de Zaragoza-CSIC, 50009 Zaragoza, Spain

[‡]Departamento de Química Física, Universidad de Málaga, Campus de Teatinos s/n, 29071 Málaga, Spain

[§]Servicio de Rayos X y Análisis por Fluorescencia, Universidad de Zaragoza, 50009 Zaragoza, Spain

Supporting Information

ABSTRACT: Chromophores where a polyenic spacer separates a 4*H*-pyranilydene or benzothiazolylidene donor and three different butenolide nitriles have been synthesized and characterized. The role of 2(*5H*)-furanones as acceptor units on the polarization and the second-order nonlinear (NLO) properties has been studied. Thus, their incorporation gives rise to moderately polarized structures with NLO responses that compare favorably to those of related compounds featuring more efficient electron-withdrawing moieties. Derivatives of the proaromatic butenolide **PhFu** show the best nonlinearities. Benzothiazolylidene-containing chromophores present less alternated structures than their pyranilydene analogues, and, unlike most merocyanines, the degree of charge transfer does not decrease on lengthening the π -bridge.



INTRODUCTION

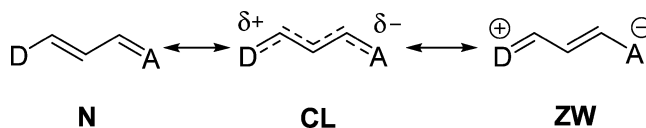
Push-pull organic chromophores, in which a π -conjugated bridge is end-capped by a donor (D) and an acceptor (A), constitute a blueprint in the search for new materials endowed with nonlinear optical (NLO) properties and have been extensively studied because of their technological and fundamental interest.¹ In such a D- π -A arrangement, efficient intramolecular charge transfer (ICT) from the donor to the acceptor takes place, and the molecules become polarized. Microscopically, the second-order nonlinearity of chromophores can be represented by the scalar product of the vector part of the hyperpolarizability tensor (β) and the dipole moment (μ).

The extent of the ICT can be finely tuned by variations of particular D, π , and A components of a push-pull molecule, and this has been demonstrated to be crucial to maximize the second-order NLO response. In this way, general structure-activity relationships have been established.²

In simple valence bond language, D- π -A systems can be represented by two extreme limiting forms: neutral (N) and zwitterionic (ZW) with an intermediate situation corresponding to the so-called “cyanine limit” (CL) (Scheme 1).

According to this model, it is possible to maximize β by optimizing the contribution of the neutral and the charge-

Scheme 1. Canonical Forms for a D- π -A System



separated canonical forms to the ground state of the molecule. This mixing can be evaluated through the bond length alternation (BLA) value, defined as the difference between the average C-C single and multiple bond lengths in the conjugated backbone.³ In chromophores with weak D and A groups, β is positive. As the molecular polarization progressively increases (for instance, by using stronger D or A ends), β increases, peaks in a positive sense, and then decreases, crosses through zero at the cyanine limit, and then becomes negative when the ground state of the molecule becomes zwitterionic. The rationalization of this behavior (Marder's plot)^{3b} has allowed the establishment of very useful guidelines for the design of NLO chromophores.⁴

Most frequently, in search of the optimization of the β value, modern push-pull molecules are equipped with strong D/A

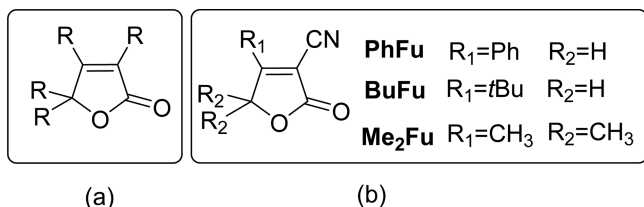
Received: September 2, 2015

Published: November 20, 2015

units, and single acceptors (like formyl, cyano, or nitro groups)⁵ are less used. However, weak acceptors could provide high nonlinearities when combined with a strong donor and an efficient π -relay.

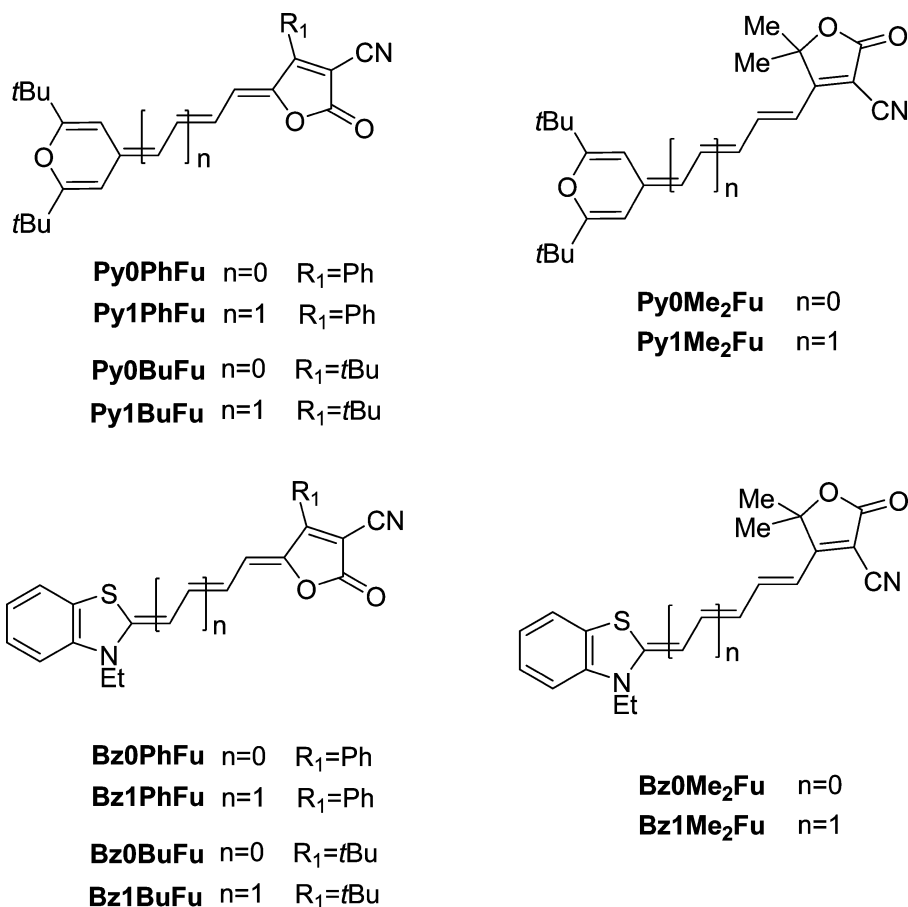
$\Delta^{\alpha,\beta}$ -Butenolides (or 2(*SH*)-furanones)⁶ (Scheme 2a) constitute an important class of natural products,⁷ among

Scheme 2. (a) General Structure of a 2,3,4,4-Tetrasubstituted But-2-ene-4-olide; and (b) Structures of But-2-ene-4-olide Nitriles Used in This Work



which the best known is vitamin C. Although they have been deeply studied because of their biological applications, this type of heterocycle has been scarcely used in the field of NLO: on the experimental side, the only studies were reported by Chang et al.,^{8a} who studied the NLO response of a merocyanine bearing a benzothiazole unit as donor. Authors indicate that this dye is a one-dimensional chromophore with an important $\mu\beta$ value measured by solvatochromic methods and, on the other hand, on a derived LB film. Theoretical calculations also confirm their NLO activity.⁸

Scheme 3. Structures of the Target Compounds



Butenolide nitriles, with a cyano group in C2 (Scheme 2b), could act as weak electron-withdrawing units and, depending on the substitution, offer a double alternative: (i) reacting by the C4 (Scheme 2b; $R_2 = \text{H}$) they would be incorporated to the chromophore as proaromatic^{4a} acceptors; (ii) reacting by the R_1 position (Scheme 2b) they would be linked to the π -spacer as nonproaromatic acceptors and could be considered as a “weak version” of the widely used 2-dicyanomethylene-3-cyano-4,5,5-trimethyl-2,5-hydrofuran (TCF) acceptor.⁹

In this context, we have turned our attention to the study of $D-\pi-A$ compounds with 2(*SH*)-furanones as electron-withdrawing moieties, having second-order NLO responses. Thus, three butenolide-type acceptors have been chosen for this work (Scheme 2b): compounds **PhFu** and **BuFu** are proaromatic acceptors and differ on the R_1 substituent, a phenyl (**PhFu**) or a *tert*-butyl group (**BuFu**). The latter have a double purpose: first, to disclose the effect of an inductive-donor and bulky substituent on the electron-withdrawing unit, and, second, to increase the solubility of the final chromophores. 2(*SH*)-Furanone **Me₂Fu** is a non proaromatic acceptor. Overall, this will allow one to evaluate the effect that the quinoid or nonquinoid character of the acceptor moiety has on the molecular polarization and on the NLO response of the final $D-\pi-A$ systems.

With the aim of ensuring an effective molecular polarization, compounds **PhFu**, **Me₂Fu**, and **BuFu** have been combined (Scheme 3) with a polyene relay and two proaromatic electron-donor moieties: 4*H*-pyranylidene¹⁰ (series **Py**) and benzothiazolylidene¹¹ (series **Bz**). The latter fragment has also been

studied as acceptor¹² or π -spacer¹³ in chromophores with NLO properties.

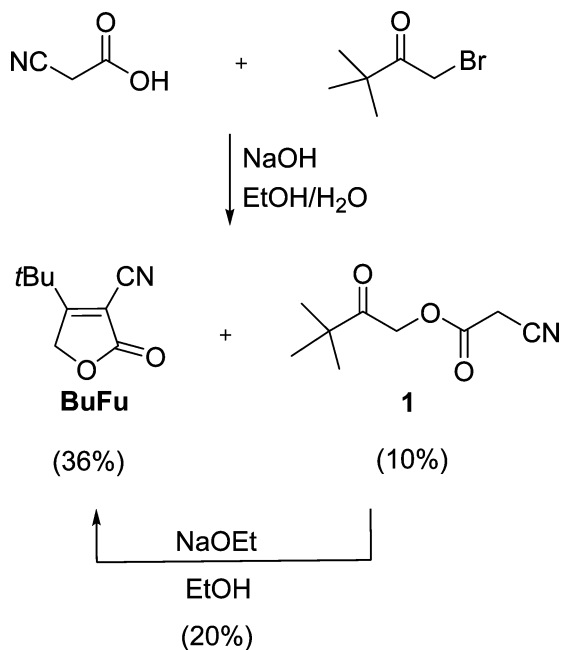
For the sake of clarity, target compounds (Scheme 3) have been named beginning with Py or Bz, to indicate the donor, followed by a number (0 or 1) that denotes the length of the π -spacer, and PhFu, Me₂Fu, BuFu that concerns the butenolide ring.

A detailed investigation of the ICT existent in these chromophores by using different techniques, together with the measurement of their $\mu\beta$ figure of merit, is presented throughout this Article.

RESULTS AND DISCUSSION

Synthesis. The synthesis of acceptors PhFu, Me₂Fu, and BuFu was previously reported^{14–16} with a different method for each butenolide. Our attempts to prepare BuFu according to a previously described method¹⁶ led to the desired compound, but not with successful yield. For this work, compound BuFu then was synthesized by following the experimental protocol used for PhFu (Scheme 4), starting from 1-bromopinacolone

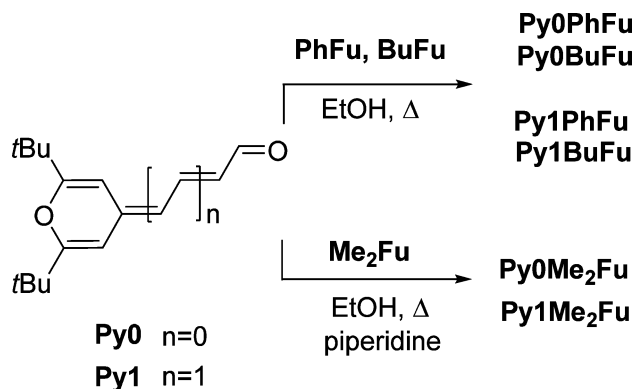
Scheme 4. Synthesis of Butenolide Nitrile BuFu



and cyanoacetic acid, and was fully characterized. During this synthesis, the corresponding oxo-cyanoacetate 1 was also isolated and characterized. Subsequent cyclization of 1 in the presence of base afforded another portion of furanone BuFu (Scheme 4).

For series Py, the Knoevenagel reaction between acceptors PhFu, Me₂Fu, and BuFu and pyranlydene-containing aldehydes Py0–Py1^{17,10b} in EtOH afforded the new D- π -A chromophores Py0(PhFu, Me₂Fu, BuFu) and Py1(PhFu, Me₂Fu, BuFu) in yields that ranged from 20% to 69% (Scheme 5). For the reactions involving furanone Me₂Fu, the addition of one drop of piperidine was needed. It is noteworthy that yields for derivatives Py0(PhFu, Me₂Fu, BuFu) were considerably higher than those for their vinylogues Py1(PhFu, Me₂Fu, BuFu). This is due to the fact that during the synthesis of the latter, small amounts of Py0(PhFu, Me₂Fu, BuFu) are formed as a consequence of a vinylene-shortening reaction that

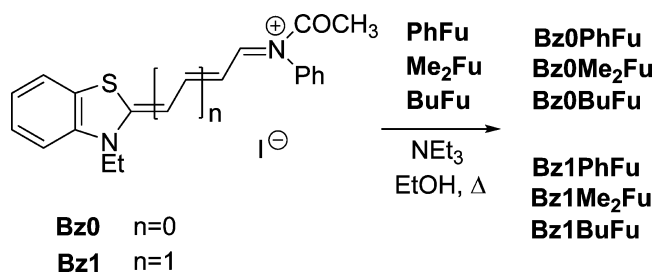
Scheme 5. Synthesis of Pyranlydene-Containing Chromophores Py0(PhFu, Me₂Fu, BuFu) and Py1(PhFu, Me₂Fu, BuFu)



has already been reported for other Knoevenagel-type reactions by us¹⁸ and other authors.¹⁹

Concerning compounds Bz0(PhFu, Me₂Fu, BuFu) and Bz1(PhFu, Me₂Fu, BuFu), they were synthesized as shown in Scheme 6, by reaction of iminium salts Bz0–Bz1²⁰ with the

Scheme 6. Synthesis of Benzothiazolylidene-Containing Chromophores Bz0(PhFu, Me₂Fu, BuFu) and Bz1(PhFu, Me₂Fu, BuFu)



corresponding acceptors PhFu, Me₂Fu, and BuFu in the presence of triethylamine. In this series, no vinylene-shortening degradation was detected.

The synthesis of compound Bz0PhFu had already been reported¹⁴ using piperidine as base, but not fully characterized. Moreover, its NLO response had been previously studied by other authors^{8a} as mentioned in the Introduction.

Structural Characterization by X-ray Crystallography.

Single crystals of compounds Py0PhFu, Py1PhFu, and Py1Me₂Fu were obtained by slow diffusion of hexane into a solution of the corresponding chromophore in CH₂Cl₂ at room temperature. Four crystallographically independent molecules are found in the asymmetric unit cell of Py0PhFu (Figure 1), while those of Py1PhFu and Py1Me₂Fu both contain a single molecule (Figure 2).

The analysis of the solid-state structures can provide useful information about how the ground electronic state polarization varies when modifying the character of the butenolide group or lengthening the spacer.

There are some main features shared by the three structures: (i) the D- π -A system is essentially planar with the following angles between the mean planes of the pyran and the butenolide rings (Py0PhFu, 17.3°, 6.0°, 16.9°, 6.0°; Py1PhFu, 5.5°; Py1Me₂Fu, 10°); (ii) the phenyl substituent in Py0PhFu–Py1PhFu is not coplanar with the butenolide

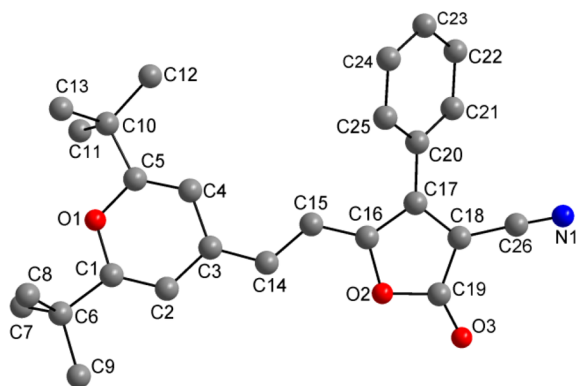


Figure 1. Molecular structure of compound **Py0PhFu**. (For clarity, only one molecule is shown. See [Figure S-38](#) for viewing the four molecules found in the asymmetric unit cell.)

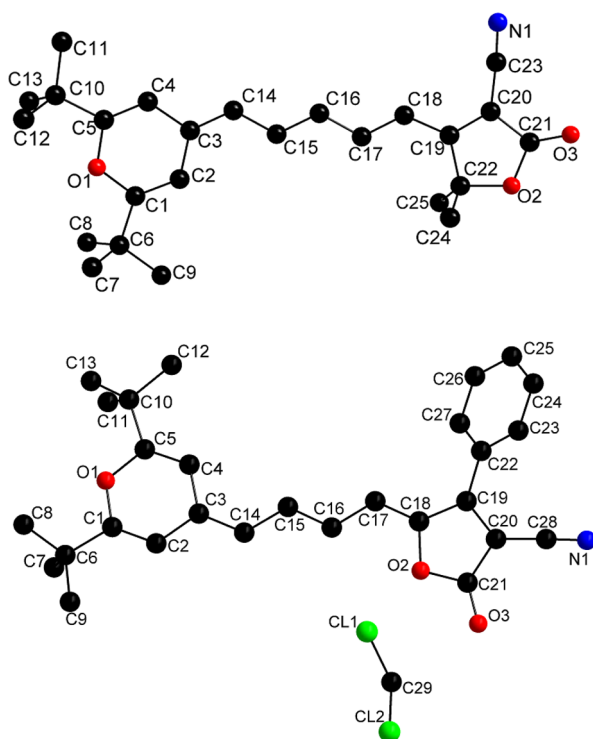
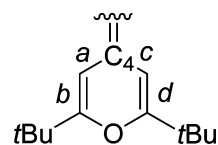


Figure 2. Molecular structures of compound **Py1PhFu**, which crystallizes with a molecule of CH_2Cl_2 (bottom), and **Py1Me₂Fu** (top).

moiety (dihedral angles: 37.4° , 45° , 36.7° and 44.6° for the four molecules in **Py0PhFu** and 33.3° in **Py1PhFu**); and (iii) the polyenic chain has an all-*trans* geometry except for the formal double bond connecting the π -spacer with the acceptor unit in **Py0PhFu–Py1PhFu**, with a *Z* configuration.

Some structural parameters of the pyranlydene ring, including BLA value along the spacer ([Figure 3](#)), reveal the ground electronic state polarization from the donor end of the chromophore to the acceptor group.

For compounds **Py0PhFu–Py1PhFu**, a shortening of C–O bond, together with a lengthening of the pyran exocyclic bond and a decreased degree of C–C bond alternation (evaluated through the parameter δr ,²¹ $\delta r = (a - b + c - d)/2$; $\delta r = 0$ for benzene and 0.10 for fully quinoid rings), was then found. Moreover, the Bird index (I_6)²² of the donor ([Figure 3](#)), used as an estimation of the aromaticity of the ring ($I_6 = 25.4$ for



Bond lengths involved in the calculation of δr

Compd	C–O ^a	C ₄ –C _{exo} ^a	δr	I_6	BLA ^a
Py0PhFu ^b	1.372	1.391	0.094	34.2	0.023
Py1PhFu	1.374	1.386	0.098	32.3	0.030
Py1Me₂Fu	1.374	1.354	0.113	27.8	0.056

^a Bond length in Å

^b Average values for the four molecules

Figure 3. Structural parameters for the pyranlydene donor and BLA values.

fully quinoid pyrans; $I_6 = 50$ for pyrylium cations^{10b}), also indicates the partial contribution of the zwitterionic form to the ground electronic state of derivatives **Py0PhFu–Py1PhFu**.

Furthermore, comparison of structural parameters ([Figure 3](#)) shows that compound **Py0PhFu** presents a more polarized structure than its vinylogue **Py1PhFu**.

Comparison with X-ray structures of merocyanines bearing other acceptors could be instructive to get more information about the ground electronic state polarization of the studied systems. For instance, analogues of **Py0PhFu/Py1PhFu** with 3-phenyl-5-isoxazolone^{10b}/1,1,3-tricyano-2-phenylpropene^{10b} or 2-dicyanomethylenethiazole,^{10c} respectively, as the acceptor end show a BLA value close to zero. This indicates that incorporation of acceptor **PhFu** leads to moderately polarized structures, and this fact may have a positive effect on the NLO behavior (see [Nonlinear Optical Properties](#)) as it places compounds **Py0PhFu–Py1PhFu**, at least in the solid state, far from the cyanine limit. In this context, the structure of **Py1PhFu** is similar to that of its recently reported 2-dicyanomethylenethiophene²³ analogue.

The structural parameters for **Py1Me₂Fu** ([Figure 3](#)) indicate a limited polarization of the donor unit given that the δr parameter and the C₄–C_{exo} bond length (C3=C14 bond in **Py1Me₂Fu**, see [Figure 2](#)) both exhibit values corresponding to a fully quinoid 4*H*-pyranlydene ring. In fact, 1.354 Å is even shorter than the C₄–C_{exo} bond in 2,2',6,6'-tetraphenylbipyranylidene (1.385 Å) taken as reference for a quinoidal derivative.²⁴ On the other hand, the BLA value for **Py1Me₂Fu** is 0.056 Å ([Figure 3](#)), which locates the chromophore in the region where β is maximized due to an optimal degree of mixing between neutral and charge-separated canonical forms.²⁵

Moreover, comparison of the structural parameters of **Py1PhFu/Py1Me₂Fu**, with a proaromatic/non proaromatic furanone as acceptor fragment, respectively, indicates that **Py1Me₂Fu** presents a more alternated structure.

Concerning series **Bz**, single crystals of derivative **Bz0PhFu** were obtained by slow diffusion of propan-2-ol into a solution of the chromophore in CH_2Cl_2 at room temperature.

Compound **Bz0PhFu** crystallizes in the monoclinic space group $P21/c$, and some of the main features of this structure are similar to those of the described above. For this compound, another X-ray structure has been previously reported, different from the structure submitted here: it claims a $P\bar{1}$ space group, incorporating a CHCl_3 crystallized molecule.²⁶ Both structures have the same geometric configurations.

In our structure, the BLA value is -0.005 \AA , indicating that this chromophore is close to the cyanine limit in the solid state, and therefore located in region C of Marder's plot.^{3b} These data also account for a more polarized structure than its analogue **Py0PhFu** (BLA = 0.023, Figure 3) pointing to a better electron-donating ability of the benzothiazole moiety as compared to that of the pyranilidene ring. This behavior is in agreement with the trend followed by octupolar merocyanine dyes designed for two-photon absorption (TPA) with these donors.²⁷

A complete description of the crystal structure is reported in the Supporting Information, section 5.

CCDC-1407292 (**Bz0PhFu**), CCDC-1407293 (**Py0PhFu**), CCDC-1407294 (**Py1Me₂Fu**), and CCDC-1407295 (**Py1PhFu**) contain the supplementary crystallographic data for this Article. These data can be obtained free of charge from The Cambridge Crystallographic Data Centre.

¹H NMR Studies. ¹H NMR spectroscopy affords valuable information about both the geometry and the ground electronic state polarization of the chromophores herein studied. Concerning their stereochemistry, analysis of ³J_{HH} coupling constants indicates an all-*trans* geometry along the spacer, with ³J_{HH} values ranging from 14.9 to 13.4 Hz for the $-\text{CH}=\text{CH}-$ bonds and from 13.1 to 11.6 Hz for the $=\text{CH}-\text{CH}=-$ bonds. This stereochemistry mimics those observed by X-ray diffraction for compounds **Py0PhFu**, **Py1PhFu**, **Py1Me₂Fu**, and **Bz0PhFu**.

Regarding the ground electronic state polarization of the studied compounds, the analysis of ΔJ values (defined as the difference between the averaged ³J_{HH} values of the double and single bonds along the polymethine chain)²⁸ for **Py1(PhFu, Me₂Fu, BuFu)**, obtained from spectra registered in CDCl_3 (1.0, 2.3, and 1.5 Hz, respectively) indicates that polarization increases in the order **Py1Me₂Fu** < **Py1BuFu** < **Py1PhFu**, which reveals the fact that quinoidal butenolides (**PhFu, BuFu**) are better electron-withdrawing groups than nonquinoidal **Me₂Fu**. For **PhFu** (with a phenyl group) and **BuFu** (with the *tert*-butyl substituent), the former presents a higher electron-withdrawing character.

For the analysis of the benzothiazolylidene derivatives, see the Supporting Information, section 3, Figure S25.

Finally, for all chromophores, the chemical shifts of the H atoms along the spacer show the typical oscillatory behavior²⁹ that reflects the alternation in the electron density of the carbon atoms to which H's are bonded: for example, for **Py1BuFu**, starting from pyranilidene donor group, in CDCl_3 5.68, 7.08, 6.59, 6.73 ppm.

Calculated Structures. The molecular geometries of all chromophores were optimized at the CPCM-M06-2X/6-31G* level in dichloromethane, starting from configurations depicted in Scheme 3, which are supported by crystallographic and spectral data. The resulting theoretical structures were nearly planar.

Analysis of natural bond orbital (NBO) atomic charge on various molecular domains (Table 1) allows a deeper understanding of the polarization of the molecules.

Table 1. Calculated NBO Charges on Various Molecular Domains from the Optimized CPCM-M06-2X/6-31G* Molecular Geometries (in CH_2Cl_2)

compd	donor	π -spacer	acceptor
Py0PhFu	+0.371	+0.005	-0.376
Py0Me₂Fu	+0.340	-0.054	-0.286
Py0BuFu	+0.340	-0.007	-0.333
Py1PhFu	+0.324	+0.027	-0.351
Py1Me₂Fu	+0.297	-0.034	-0.263
Py1BuFu	+0.297	+0.008	-0.305
Bz0PhFu	+0.465	-0.059	-0.406
Bz0Me₂Fu	+0.432	-0.131	-0.301
Bz0BuFu	+0.436	-0.072	-0.364
Bz1PhFu	+0.421	-0.043	-0.378
Bz1Me₂Fu	+0.394	-0.114	-0.280
Bz1BuFu	+0.397	-0.067	-0.330

In general, the positive charge is concentrated on the donor ring and the negative charge on the acceptor moiety, although in the **Bz** series, the π -spacer supports a slight negative charge, more important for derivatives **Me₂Fu**.

For both series (**Py** and **Bz**), comparison of compounds that only differ in the acceptor group shows that polarization of the chromophores increases in the order **Me₂Fu** < **BuFu** < **PhFu**, in agreement with ¹H NMR data and X-ray studies (**Py1PhFu/Py1Me₂Fu**), thus confirming the higher electron-withdrawing ability for butenolide **PhFu**.

For a given D/A pair, lengthening the conjugated spacer with a vinylene unit leads to a decrease in the charge of the end groups and, in consequence, to more alternated structures, in line with the findings from the X-ray analysis (**Py0PhFu/Py1PhFu**).

Finally, comparison of the charges between analogous chromophores of the **Py** and **Bz** series shows that the latter are more polarized than their **Py** analogues, indicating a major contribution of the zwitterionic form to the ground state, as it has been shown by the crystallographic study of **Py0PhFu/Bz0PhFu**.

Electrochemistry. The redox properties of target chromophores together with acceptors **PhFu, Me₂Fu, and BuFu** were studied by cyclic voltammetry (CV) in CH_2Cl_2 , and the results are gathered in Table 2.

Voltammograms for acceptors **PhFu, Me₂Fu, and BuFu** show an irreversible reduction wave. Values of E_{red} depend on the type of the furanone. Thus, the nonproaromatic acceptor **Me₂Fu** presents the highest $|E_{\text{red}}|$ data. For proaromatic acceptors **PhFu** and **BuFu**, the presence of a *tert*-butyl group in C4 implies a lower electron-withdrawing ability with higher $|E_{\text{red}}|$ for **BuFu** as compared to **PhFu**.

All D- π -A systems show one oxidation and one reduction wave corresponding to the donor moiety and the acceptor unit, respectively. The reduction process for the series **Py** is reversible. When E_{red} data are compared in both **Py** and **Bz** series, results follow the same trend encountered for the isolated acceptors; that is, the reduction process is easier in the order: systems **Me₂Fu** < systems **BuFu** < systems **PhFu**, thus confirming the superior electron-withdrawing effect of acceptor **PhFu**, in agreement with ¹H NMR study, crystal structures (**Py1PhFu/Py1Me₂Fu**), and theoretical data. Inspection of calculated E_{LUMO} data indicates that derivatives of acceptor **PhFu** have the lowest values. On the other hand, E_{ox} values are also influenced by the acceptor fragment, with compounds

Table 2. Electrochemical Data^a and E_{HOMO} and E_{LUMO} Values Theoretically Calculated^b

compd	E_{ox} (V)	E_{red} (V)	E_{HOMO} (eV)	E_{LUMO} (eV)
PhFu		-1.23		
Me ₂ Fu		-1.85		
BuFu		-1.74		
Py0PhFu	+0.89	-0.98 ^{c,d}	-6.56	-2.35
Py0Me ₂ Fu	+0.93	-1.17 ^{c,e}	-6.61	-2.10
Py0BuFu	+0.86	-1.09 ^{c,d}	-6.51	-2.19
Py1PhFu	+0.64	-0.82 ^{c,f}	-6.29	-2.49
Py1Me ₂ Fu	+0.64	-1.02 ^{c,f}	-6.33	-2.26
Py1BuFu	+0.59	-0.94 ^{c,e}	-6.25	-2.34
Bz0PhFu	+0.84	-1.15	-6.46	-2.18
Bz0Me ₂ Fu	+0.79	-1.38	-6.50	-1.90
Bz0BuFu	+0.82	-1.31	-6.41	-2.01
Bz1PhFu	+0.56	-1.02	-6.20	-2.36
Bz1Me ₂ Fu	+0.55	-1.20	-6.23	-2.12
Bz1BuFu	+0.48	-1.12	-6.16	-2.20

^a10⁻³ M in CH₂Cl₂ versus Ag/AgCl (3 M KCl), glassy carbon working electrode, Pt counter electrode, 20 °C, 0.1 M NBu₄PF₆, 100 mV s⁻¹ scan rate. Ferrocene internal reference $E^{1/2} = +0.46$ V ($\Delta E_p = 0.13$ V). ^bCalculated at the CPCM-M06-2X/6-311+G(2d,p)//CPCM-M06-2X/6-31G* level in CH₂Cl₂. ^cReversible reduction wave ($E^{1/2}$). ^d $\Delta E_p = 0.13$ V. ^e $\Delta E_p = 0.12$ V. ^f $\Delta E_p = 0.11$ V.

derived from BuFu (except Bz0BuFu) the most easily oxidized. E_{HOMO} data are in agreement with this observed trend.

Moreover, for a given acceptor, it can be seen that both oxidation and reduction processes become easier on chain lengthening (for example, Py0PhFu/Py1PhFu; Bz0PhFu/Bz1PhFu), pointing to a weaker interaction between the donor and acceptor ends. In line with this analysis, compounds 0 show higher calculated gaps than their vinyllogues 1.

Comparison of compounds Py with their analogues of series Bz shows lower (higher) oxidation (reduction) potentials for the latter, pointing to the higher electron-donating ability of the benzothiazole moiety. This result is in agreement with the literature data.³⁰ Furthermore, the observed trends in E_{ox} and E_{red} are also confirmed by theoretical calculations, which show that both E_{HOMO} and E_{LUMO} values increase on passing from pyran derivatives Py to their benzothiazole Bz counterparts.

Vibrational Spectroscopy. Infrared (IR) spectroscopy can afford useful information about the degree of ground-state polarization of the merocyanines herein studied.^{10c,23,31} Thus, the stretching vibration frequencies of the C≡N and C=O bonds are sensitive to the increasing electron density on them, downshifting upon ground-state polarization. Indeed, taking the isolated acceptors PhFu, Me₂Fu, and BuFu as references

(Table 3), the $\nu(\text{C}\equiv\text{N})$ and $\nu(\text{C}=\text{O})$ frequency values of Py0(PhFu,Me₂Fu,BuFu), Py1(PhFu,Me₂Fu,BuFu), Bz0(PhFu,Me₂Fu,BuFu), and Bz1(PhFu,Me₂Fu,BuFu) appear at significantly lower frequencies, affirming the polarization from the donor to the butenolide group.

Table 3 reveals two different trends concerning the dependence of $\nu(\text{C}\equiv\text{N})$ on chain lengthening. Thus, for pyranilidene-containing chromophores (Py series), increasing the length of the polyenic spacer gives rise to a frequency upshift of $\nu(\text{C}\equiv\text{N})$ (also for $\nu(\text{C}=\text{O})$ values), except for Py0Me₂Fu and Py1Me₂Fu ($\nu(\text{C}\equiv\text{N})$). This reveals a decreased polarization (and zwitterionic character) for the longer derivatives 1, in agreement with calculated data and X-ray (Py0PhFu/Py1PhFu).

On the other hand, lengthening the spacer in the series Bz leads to a frequency downshift of the $\nu(\text{C}\equiv\text{N})$ vibration (compounds Bz0Me₂Fu–Bz1Me₂Fu have similar values), which suggests a higher zwitterionic character for the longer derivatives. This behavior may be related to the more extended conjugation path, which facilitates polarization of the π system toward the butenolide end, and, although this trend is uncommon, some examples are reported.^{10c,11e,32}

The lower frequencies of both $\nu(\text{C}\equiv\text{N})$ and $\nu(\text{C}=\text{O})$ bands in series Bz as compared to those of series Py (derivatives of furanone Me₂Fu do not fulfill this trend for the C≡N bond, see below discussion about Raman spectroscopy) show the stronger electron-donating ability of the benzothiazole group in relation to the pyranilidene one, as disclosed by computational studies and X-ray (Py0PhFu/Bz0PhFu).

Figure 4 shows the Raman spectra of the studied compounds. The $\nu(\text{C}\equiv\text{N})$ in compound Py0PhFu appears at 2214 cm⁻¹ and shifts to 2210 cm⁻¹ in Bz0PhFu, reaffirming the greater electron donor ability of the latter. The corresponding $\nu(\text{C}=\text{O})$ appears at 1736 cm⁻¹ in Py0PhFu and 1708 cm⁻¹ in Bz0PhFu. This frequency downshift on Bz0PhFu is related to a larger contribution of the enolic structure C upon charge polarization (Scheme 7), which is consistent with the five-membered ring viewed as an aromatic furan and substituted at the β position (α in the furanone ring) by the cyano group. This aromaticity gain upon polarization favors a greater delocalization of the charge on the carbonyl group. In this regard, the cyano is placed in a cross conjugated fashion constraining its electron-withdrawal character.

On increasing the length of the C=C/C–C spacer from Bz0PhFu to Bz1PhFu, the $\nu(\text{C}\equiv\text{N})$ band shifts as 2210 cm⁻¹ → 2202 cm⁻¹, whereas the $\nu(\text{C}=\text{O})$ Raman band is not detected, likely due to the strong enolic character that

Table 3. Infrared Data^a

compd	$\nu(\text{C}\equiv\text{N})$	$\nu(\text{C}=\text{O})$	compd	$\nu(\text{C}\equiv\text{N})$	$\nu(\text{C}=\text{O})$
PhFu	2231	1752			
Me ₂ Fu	2239	1769			
BuFu	2238	1776			
Py0PhFu	2213	1739	Bz0PhFu	2207	1722
Py0Me ₂ Fu	2206	1738	Bz0Me ₂ Fu	2210	1723
Py0BuFu	2215	1746	Bz0BuFu	2209	1720
Py1PhFu	2217	1742	Bz1PhFu	2200	1729
Py1Me ₂ Fu	2201	1742	Bz1Me ₂ Fu	2213	1739
Py1BuFu	2219	1749	Bz1BuFu	2191	1702

^aMeasured on nujol suspension; data in cm⁻¹.

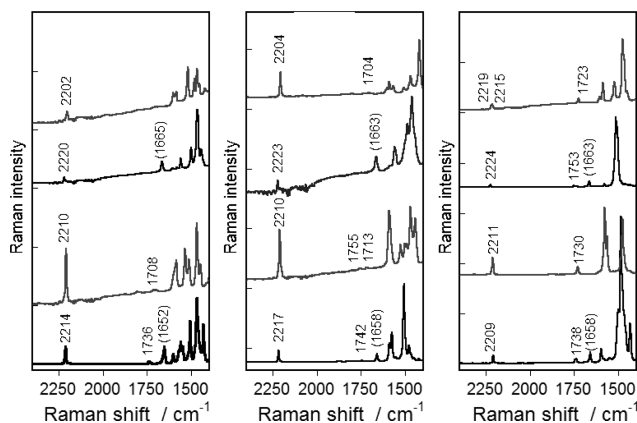


Figure 4. 1064 nm FT-Raman spectra in the solid state of the studied compounds. From the bottom to the top, left: **Py0PhFu**, **Bz0PhFu**, **Py1PhFu**, and **Bz1PhFu**. Middle: **Py0BuFu**, **Bz0BuFu**, **Py1BuFu**, and **Bz1BuFu**. Right: **Py0Me₂Fu**, **Bz0Me₂Fu**, **Py1Me₂Fu**, and **Bz1Me₂Fu**.

dramatically decreases its Raman intensity, as is typical of alcoholate compounds. This situation is in agreement with an important increase of the contribution of the C type canonical form (Scheme 7) for compound **Bz1PhFu**, further indicating that, by lengthening the π -spacer in series **Bz**, a more polarized structure results. In contrast, in **Py** series, given their weaker electron-donating character, a frequency upshift behavior is observed. Moreover, the bands at 1652 (**Py0PhFu**) and 1665 (**Py1PhFu**) cm^{-1} are due to the $\nu(\text{C}=\text{C})$ modes in the pyranilidene moieties.

The replacement of the phenyl group in β position of the furanone by a *tert*-butyl one does not change the main tendencies (downshifts of the $\nu(\text{C}\equiv\text{N})$ and $\nu(\text{C}=\text{O})$ Raman frequencies, on passing from **Py0BuFu** to **Bz0BuFu** and from **Bz0BuFu** to **Bz1BuFu**) observed for the phenyl-substituted series. For derivatives **0**, different trends depending on the donor are observed: for pyranilidene derivatives, frequencies upshift from **Py0PhFu** to **Py0BuFu**, due to the strong steric

crowding that the *tert*-butyl group exerts on the vinylic bridge, which weakens the donor–acceptor coupling (Figure 5).

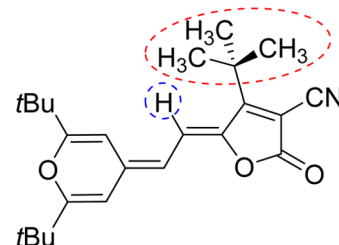


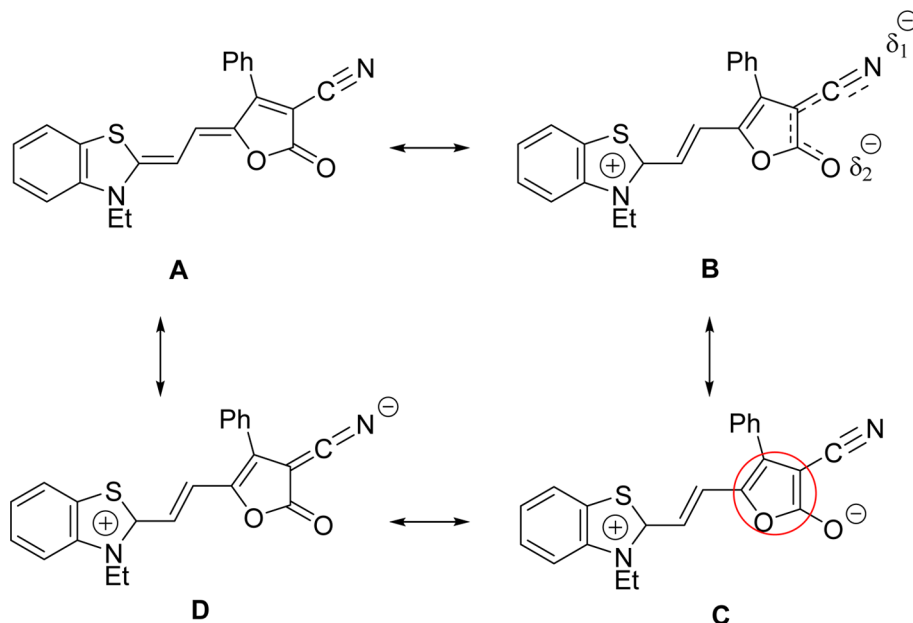
Figure 5. Crowding effect of the *tert*-butyl group that decreases the molecular polarization (chromophore **Py0BuFu**).

On the other hand, for benzothiazolylidene systems **Bz0PhFu** and **Bz0BuFu**, the frequencies scarcely change.

For chromophores bearing butenolide **Me₂Fu**, a canonical form similar to C in Scheme 7 no longer exists, and the acceptor part of the molecule can be viewed as an acceptor with a cyano and an ester group, placed one after the other, in a cross-conjugated fashion, and therefore competing for the negative charge. Given the disposition of the two groups, the cyano, with a slightly stronger electron-withdrawing character than the ester, should have a preferential situation to drain charge from the bridge. This can be the reason for the lower frequency for the $\nu(\text{C}\equiv\text{N})$ band in **Py0Me₂Fu** (2209 cm^{-1}) as compared to **Py0PhFu** (2214 cm^{-1}). On the other hand, the $\nu(\text{C}=\text{O})$ frequencies scarcely change due to the lack of enolic character (form C in Scheme 7), which is compensated by the inductive effect of the oxygen in the ester. These two trends are also observed in the IR data (Table 3).

For derivative **Bz0Me₂Fu**, the $\nu(\text{C}=\text{O})$ bands undergo significant upshifts regarding **Bz0PhFu** or **Bz0BuFu**, which further reaffirm the isolation of the carbonyl groups in a position unaffected by the charge polarization (fully gathered by the nitriles).

Scheme 7. Canonical Forms upon Charge Polarization for Chromophore **Bz0PhFu**



Overall, the replacement of **PhFu** and **BuFu** units as acceptors by furanone **Me₂Fu** involves a decrease in the polarization of the final chromophores.

A study of the frequency behavior of the $\nu(\text{C}\equiv\text{N})$ and $\nu(\text{C}=\text{O})$ bands in the oxidized and reduced forms according to the redox processes in the CV is also carried out and presented in the [Supporting Information, section 6](#).

UV–Vis Spectroscopy. The UV–vis absorption data of push–pull systems in solvents with different polarity are collected in [Table 4](#). All chromophores show very strong and

Table 4. UV–Vis Data^a

compd	λ_{max} (log ϵ) 1,4-dioxane	λ_{max} (log ϵ) CH ₂ Cl ₂	λ_{max} (log ϵ) DMF
Py0PhFu	503 (sh)	519 (sh)	518 (sh)
	536 (4.71)	559 (4.79)	558 (4.79)
	568 (sh)	591 (4.81)	597 (4.85)
Py0Me₂Fu	491 (4.56)	499 (sh)	498 (sh)
	515 (4.57)	532 (4.69)	529 (4.70)
	553 (sh)	568 (4.57)	563 (sh)
Py0BuFu	487 (sh)	505 (sh)	506 (sh)
	513 (4.68)	539 (4.79)	544 (4.75)
	554 (sh)	573 (sh)	580 (sh)
Py1PhFu	589 (4.63)	585 (sh)	589 (sh)
		635 (4.73)	638 (4.71)
		684 (sh)	692 (4.63)
Py1Me₂Fu	538 (4.63)	585 (4.70)	575 (4.69)
		644 (sh)	
Py1BuFu	551 (4.47)	599 (4.50)	598 (4.47)
			679 (sh)
Bz0PhFu	529 (sh)	538 (sh)	538 (sh)
	566 (4.80)	576 (5.10)	579 (5.10)
Bz0Me₂Fu	521 (4.74)	523 (sh)	524 (sh)
	541 (4.78)	553 (4.93)	559 (4.97)
Bz0BuFu	521 (sh)	529 (4.75)	533 (4.72)
	550 (4.85)	564 (5.10)	567 (5.67)
Bz1PhFu	611 (sh)	628 (sh)	634 (sh)
	642 (4.59)	678 (5.00)	687 (5.23)
Bz1Me₂Fu	585 (4.46)	596 (sh)	596 (sh)
		634 (4.78)	644 (4.84)
Bz1BuFu	594 (4.67)	618 (4.86)	623 (sh)
		656 (5.00)	669 (5.12)

^aAll λ_{max} data in nanometer.

broad electronic absorption bands within the visible region, with structured bands in some of the solvents studied. (See spectra in the [Supporting Information](#).)

Electron densities related to frontier orbitals (see topologies for **Py1BuFu** chosen as the model compound in [Figure 6](#) and those for the rest of the chromophores in the [Supporting Information](#)) are mainly supported by the donor unit and its nearest polyenic fragment for the HOMO, and by the butenolide ring in the case of LUMO.

TD-DFT calculations (CPCM-M06-2X/6-311+G(2d,p)//CPCM-M06-2X/6-31G* level in CH₂Cl₂) describe the first excited state as a consequence of a one-electron transition from the HOMO to the LUMO. The large HOMO–LUMO overlap is responsible for the strength of the absorption bands.

Comparison of series **0** and **1** indicates that the λ_{max} values increase on lengthening the spacer, an effect that is more accentuated in CH₂Cl₂ or DMF than in the less polar 1,4-dioxane. Taking as model pairs **Py0PhFu/Py1PhFu** and

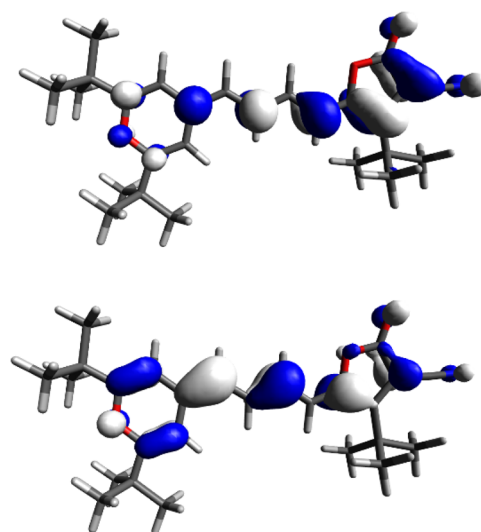


Figure 6. Illustration of the HOMO (bottom) and LUMO (top) of compound **Py1BuFu**.

Bz0PhFu/Bz1PhFu, this augmentation reaches ~ 100 nm,³³ pointing to weakly alternated structures, more polarized in the case of **Bz** derivatives (102 nm, 0.32 eV in CH₂Cl₂; 108 nm, 0.34 eV in DMF) than in **Py** systems (0.29 eV both in CH₂Cl₂ and DMF). This trend is in agreement with other experimental techniques (IR, Raman, CV, **Py0PhFu/Bz0PhFu** X-ray) and calculated NBO charges.

When different furanones are compared, λ_{max} decreases in the following order: **PhFu** > **BuFu** > **Me₂Fu**. This behavior can be explained, on the one hand, by the character (quinoid or nonquinoid) of the acceptor moiety. Thus, the presence of the quinoid ring causes a red shift of the maximum absorption wavelength in derivatives **PhFu**, **BuFu** when compared to their analogues **Me₂Fu** (e.g., 23 nm (0.08 eV) for **Py0PhFu/Py0Me₂Fu** and 5 nm (0.02 eV) for **Py0BuFu/Py0Me₂Fu**, both in CH₂Cl₂). On the other hand, the replacement of the phenyl ring in compounds **PhFu** for a *tert*-butyl group in derivatives **BuFu** gives rise to a hypsochromic shift (e.g., 85 nm (0.26 eV) for **Py1PhFu/Py1BuFu** and 22 nm (0.06 eV) for **Bz1PhFu/Bz1BuFu**, both in CH₂Cl₂). The same effect was observed for cyanine dyes bearing a 4*H*-pyran-4-ylidene moiety.³⁴ The order above-mentioned suggests a parallel decrease in the corresponding acceptor strengths (**PhFu** > **BuFu** > **Me₂Fu**), in line with the results of ¹H NMR spectroscopy, theoretical data, and CV.

In general, derivatives of **Bz** series present λ_{max} values lower than their **Py** analogues,²⁷ although for systems **1** this trend is not observed for all of the solvents studied. Moreover, **Bz** systems show larger ϵ values than their **Py** equivalents, and for some solvents, values beyond 10⁵ were found, in agreement with other benzothiazolylidene- π -A chromophores previously reported.^{11c,e,27,35}

Concerning the dependence of the band position on solvent polarity, positive solvatochromism in low polarity solvents (cf., dioxane and CH₂Cl₂) is observed for all chromophores. On the other hand, when data in CH₂Cl₂ and DMF are compared, the bathochromic shift encountered becomes smaller for derivatives **PhFu/BuFu**, whereas for compounds **Me₂Fu**, solvatochromism found depends on the donor unit: slightly negative for **Py** derivatives³⁶ and positive for **Bz** systems.

Nonlinear Optical Properties. The second-order nonlinear optical properties of chromophores herein studied were measured by electric field-induced second harmonic generation (EFISHG) in dichloromethane at 1907 nm, and the zero-frequency $\mu\beta_0$ values were calculated by using the two-level model.³⁷ In the case of the benzothiazolidene systems (series **Bz**), the lowest energy absorption band, which is the more intense one for each compound, has been used. Given that for derivatives of **Py** series the lowest energy bands in some of the spectra became weak shoulders (indistinguishable in some of the longest compounds), to compare $\mu\beta_0$ values in this series, the high intensity central band has been considered (Table 5).

Table 5. Experimental and Calculated NLO Properties

compd	$\mu\beta^a$ (10^{-48} esu)	$\mu\beta_0^b$ (10^{-48} esu)	$\mu\beta^c$ (10^{-48} esu)
PyOPhFu	950	575	521
PyOMe ₂ Fu	800	510	395
PyOBuFu	850	530	499
Py1PhFu	2850	1420	2125
Py1Me ₂ Fu	2100	1190	1798
Py1BuFu	1800	990	1801
BzOPhFu	560	325	580
BzOMe ₂ Fu	520	320	477
BzOBuFu	<i>d</i>		531
Bz1PhFu	3300	1440	2136
Bz1Me ₂ Fu	2900	1430	1838
Bz1BuFu	2600	1210	1797

^a $\mu\beta$ values determined in CH₂Cl₂ at 1907 nm (experimental uncertainty less than $\pm 15\%$, except for **BzOPhFu**–**BzOMe₂Fu** ($\sim 20\%$)). ^bExperimental $\mu\beta_0$ values in CH₂Cl₂ calculated using the two-level model. ^cCalculated at the HF/6-31G*//CPCM-M06-2X/6-31G* level in CH₂Cl₂. ^dFor this compound, a reliable value cannot be provided due to its instability in CH₂Cl₂ during the time of measurements.

For the sake of comparison, Disperse Red 1, a common benchmark for organic NLO chromophores shows a $\mu\beta_0$ value of ca. 490×10^{-48} and 425×10^{-48} esu in CH₂Cl₂ and DMF, respectively, under the same experimental conditions.

As it has been already observed for other NLO-chromophores previously studied, lengthening the polyenic chain by a single vinylene unit gives rise to an important increase in the NLO response, which is remarkably pronounced for series **Bz**: $\mu\beta_0(\text{Bz1PhFu})/\mu\beta_0(\text{BzOPhFu}) = 4.4$ and $\mu\beta_0(\text{Bz1Me}_2\text{Fu})/\mu\beta_0(\text{BzOMe}_2\text{Fu}) = 4.5$.

Regarding the influence of acceptor structure on the NLO properties of the studied chromophores, derivatives of the proaromatic butenolide nitrile **PhFu** have the best NLO responses (for **BzOPhFu**–**BzOMe₂Fu** almost the same value was obtained).

Comparison of analogous compounds in **Py** and **Bz** series reveals that, for derivatives **0**, pyranilidene-containing chromophores show higher $\mu\beta_0$ values than their related benzothiazolidene systems. Different experimental techniques (e.g., IR, Raman, CV) showed a more polarized character for benzothiazolidene chromophores, due to the higher electron-donating ability of the benzothiazole moiety as compared to the pyran one. Thus, the change **Py** → **Bz** in the more polarized shorter derivatives **0** results in a decreased NLO response, approaching the region B/C of the Marder's plot.^{3b} For **1** derivatives, NLO responses are similar for **Py** and **Bz** systems

(with furanone **PhFu**) or even higher for the latter (with acceptors **Me₂Fu** and **BuFu**).

Measurements in DMF were also performed for model compounds **Py1PhFu** and **Py1Me₂Fu**. The following experimental values (10^{-48} esu) were found: chromophore **Py1PhFu**, 1700 ($\mu\beta$), 700 ($\mu\beta_0$); chromophore **Py1Me₂Fu**, 910 ($\mu\beta$), 530 ($\mu\beta_0$). Results show a decline of $\mu\beta_0$ in both cases, as compared to those measured in dichloromethane (Table 5), indicating that these systems are left-handed chromophores (A/B region), with the neutral form predominating in this solvent polarity range.

The calculated $\mu\beta_0$ values (HF/6-31G*, Table 5) are in reasonably good consonance with the experimental ones, and they essentially reproduce the trends experimentally observed in terms of the effects of the acceptor **PhFu** and the length of the polyenic chain. Concerning the influence of the donor group, theoretical calculations do not predict the experimental observed effects for series **0**, although differences are generally small.

Finally, it could also be instructive to compare the NLO properties of the compounds herein reported to those of related derivatives featuring other acceptor moieties, including those previously mentioned in the X-ray section (see Figures 7 and 8 and Table 6).

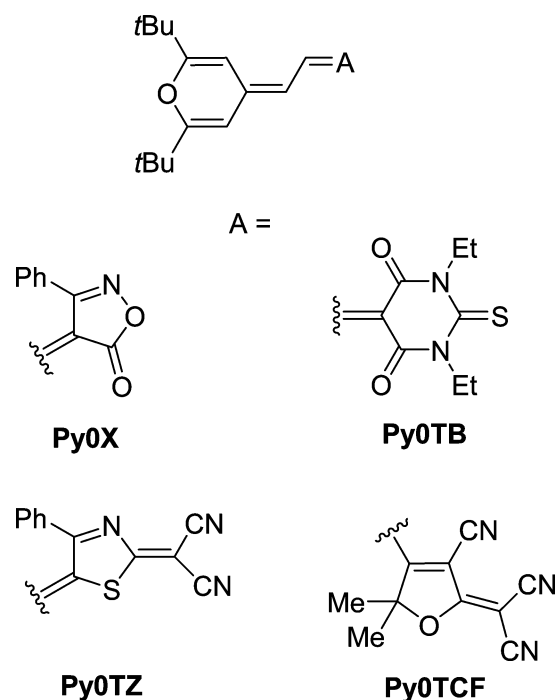


Figure 7. Structures of chromophores related to series **Py0** previously reported.

Thus, the analogue of **Py0PhFu** with 3-phenyl-5-isoxazolone as acceptor,^{10b} **Py0X**, shows a lower $\mu\beta_0$ value than **Py0PhFu**, in agreement with a more polarized structure in solution, apart from the solid state (see X-ray section). Other chromophores with powerful electron-withdrawing ends also have lower nonlinearities than **Py0PhFu**, even negative figure of merit, as in the case of the thiobarbiturate derivative **Py0TB**.^{10b}

In the same way, **Py1triCN** with 1,1,3-tricyano-2-phenylpropene^{10b} has a lower response than **Py1PhFu**, in line with a

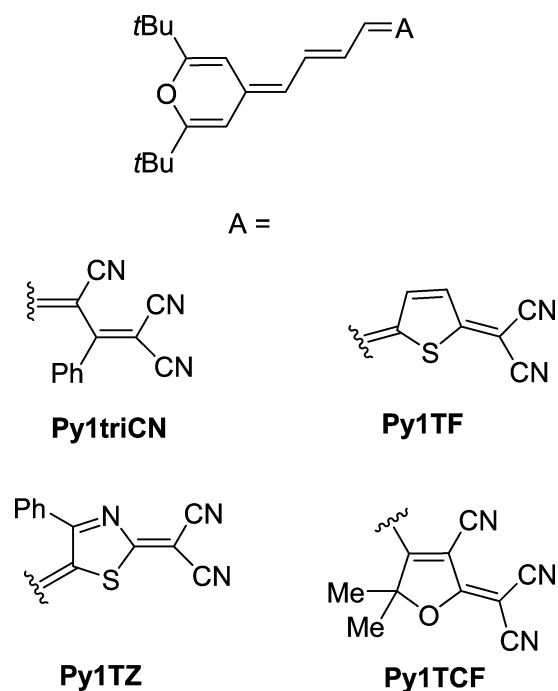


Figure 8. Structures of chromophores related to series Py1 previously reported.

Table 6. NLO Properties for Chromophores Related to Series Py

compd	ref	$\mu\beta_0^a$ (10^{-48} esu)	λ_{\max}^b (nm)
Py0X	10b	+64	
Py0TB	10b	-60	
Py0TZ	10c	-450	
Py0TCF	10b	+310	592, 639
Py1triCN	10b	+670	
Py1TF	23	+1370	658, 709, 788
Py1TZ	10c	-1010	
Py1TCF	10b	+1520	675, 740

^aExperimental $\mu\beta_0$ values in CH_2Cl_2 calculated using the two-level model from $\mu\beta$ measured by EFISHG at 1907 nm. ^bIn CH_2Cl_2 .

less alternated structure in solution (also in the solid state, as disclosed by X-ray crystallography).

Series with a 2-dicyanomethylenethiazole moiety^{10c} as the end group (Py0TZ, Figure 7 and Py1TZ, Figure 8) show negative values of $\mu\beta_0$, being essentially zwitterionic molecules that show negative solvatochromism. Nevertheless, absolute values are slightly lower as compared to those of Py0PhFu and Py1PhFu, respectively.

As it has been stated in the X-ray section, Py1PhFu and its equivalent with 2-dicyanomethylenethiophene²³ Py1TF have similar structures, and it is noteworthy that Py1PhFu, while being more transparent (Table 4), shows even slightly higher NLO response.

The pyrylidene-derived Fischer carbene complexes reported by Caro,^{10a,38} with the same length of the π -relay as the chromophores herein studied, show lower $\mu\beta_{1907}$ values than those of compounds Py0(PhFu, Me₂Fu, BuFu) and Py1(PhFu, Me₂Fu, BuFu).

On the other hand, as it has been mentioned in the Introduction, furanone Me₂Fu can be viewed as a “weak version” of the efficient TCF acceptor, and thus derivatives

Py0Me₂Fu and Py1Me₂Fu can be compared to their previously reported analogues with TCF,^{10b} Py0TCF and Py1TCF, respectively (Figures 7 and 8). For the shorter derivatives 0, and in consequence, with more polarized structures, a higher nonlinearity, which is accompanied by a hypsochromic shift of the absorption bands, is found for Py0Me₂Fu. For derivatives 1, with less polarized structures, compound Py1TCF, bearing the stronger acceptor, shows a higher NLO response, but Py1Me₂Fu is also more transparent (Table 4).

Chromophores of series Bz show positive figure of merit $\mu\beta_0$, contrary to their equivalents with 2-dicyanomethylenethiazole as acceptor.^{11e} The latter are right-handed chromophores, with a predominantly zwitterionic form for their ground electronic state. Although these were measured in DMSO due to their limited solubility in CH_2Cl_2 , the qualitative experimental results in the latter solvent also pointed to negative nonlinearities. Considering the use of different solvents, values for compounds Bz0(PhFu, Me₂Fu, BuFu) and Bz1(PhFu, Me₂Fu, BuFu) are similar or even higher in absolute values.

Further comparisons with benzothiazolylidene chromophores bearing other acceptors are somewhat restricted by the different experimental setups used in the measurement of the corresponding second-order NLO properties (hyper Raleigh scattering (HRS) as technique, other laser wavelength and/or other solvents)^{11b,c,32,39} or by the structure of merocyanine featuring a quite different π -spacer.^{11d}

Thus, in short, the NLO properties of furanone-containing merocyanines herein studied compare favorably to those of related chromophores bearing more efficient acceptor units.

CONCLUSION

$\Delta^{\alpha\beta}$ -Butenolides (or 2(5H)-furanones) have been used as acceptor ends in the synthesis of D- π -A systems with second-order NLO properties. All derivatives exist as a resonance hybrid of the neutral and zwitterionic forms, with different molecular polarization (and thus different properties), depending on the donor unit and the butenolide fragment.

X-ray crystallography, NMR data, and calculated NBO charges reveal that polarization of the chromophores studied increases in the order: systems Me₂Fu < systems BuFu < systems PhFu. Moreover, derivatives of proaromatic butenolide PhFu show the easiest reduction process and the highest absorption wavelength.

The benzothiazolylidene moiety has a better electron-donating ability as compared to that of the pyrylidene ring, as disclosed by X-ray studies, theoretical data, IR, Raman, and CV. This fact gives rise to a more effective polarization for chromophores of Bz series with an important contribution, for compounds bearing the proaromatic furanones PhFu, BuFu, of the canonical form in which furan gets aromatic. Furthermore, unlike most D- π -A systems, the degree of ICT in derivatives Bz increases on lengthening the π -spacer, as revealed by IR and Raman spectroscopies.

All compounds display positive $\mu\beta_0$ values, showing chromophores endowed with the proaromatic butenolide PhFu as acceptor moiety the best NLO responses. The change Py \rightarrow Bz results in lower second-order nonlinearities for derivatives 0, due to the more polarized structures for derivatives Bz. Incorporation of furanones PhFu, Me₂Fu, and BuFu leads to moderately polarized structures with higher NLO responses (accompanied sometimes by a better transparency) when compared to other chromophores bearing more efficient acceptors. Taking these data into account, 2(5H)-

furanones become suitable acceptor moieties for the preparation of novel structures with an effective polarization and upgraded second-order NLO responses.

EXPERIMENTAL SECTION

General Information. See the Supporting Information.

Starting Materials. Compounds **PhFu**,¹⁴ **Py0**,¹⁷ **Py1**,^{10b} **Bz0**,²⁰ and **Bz1**²⁰ were prepared as previously described. Acceptor **Me₂Fu** was prepared by following the same procedure reported for the corresponding analogue with methyl and ethyl groups in **C5**.^{15b}

4-tert-Butyl-2-oxo-2,5-dihydrofuran-3-carbonitrile (BuFu). 1-Bromopinacolone (2 mL, 14.9 mmol) and cyanoacetic acid (1.26 g, 14.9 mmol) were added to a solution of NaOH (0.60 g, 14.9 mmol) in ethanol/water (22 mL/5 mL) under an argon atmosphere. The reaction mixture was heated at reflux for 6 h 30 min (TLC monitoring). The final red solution was evaporated and the crude product dissolved in EtOAc (20 mL). The organic layer was washed with water (2 × 10 mL), dried over MgSO₄, and evaporated. The resulting orange oil was purified by flash chromatography (silica gel) with CH₂Cl₂ as the eluent, obtaining first compound **BuFu** (4-tert-butyl-2-oxo-2,5-dihydrofuran-3-carbonitrile: 884 mg, 36%) as a yellow oil, which solidified on standing, then **1** (3,3-dimethyl-2-oxobutyl cyanoacetate: 317 mg, 10%) as a yellowish solid. A second fraction of compound **BuFu** was obtained by cyclization of **1** as follows: 3,3-dimethyl-2-oxobutyl cyanoacetate **1** (317 mg, 1.73 mmol) was added to a solution of Na (20 mg, 0.87 mmol) in EtOH (2 mL) under an argon atmosphere. The mixture was stirred for 24 h turning from orange to red. HCl 1 N (2.9 mL, 2.9 mmol) was added, the aqueous layer was extracted with CH₂Cl₂ (3 × 10 mL), and the resulting organic layer was dried over MgSO₄ and evaporated. The crude oil was purified by flash chromatography (silica gel) with CH₂Cl₂/hexane 9.5:0.5 as the eluent to give **BuFu** (57 mg, 20%).

4-tert-Butyl-2-oxo-2,5-dihydrofuran-3-carbonitrile (BuFu). Mp 60–63 °C (ref 16, mp 64 °C). ¹H NMR (400 MHz, CDCl₃): δ = 4.98 (s, 2H), 1.41 ppm (s, 9H). ¹³C NMR (75 MHz, CDCl₃): δ = 188.2, 168.0, 111.1, 110.0, 71.1, 35.4, 28.4 ppm. IR (neat): $\bar{\nu}$ = 2975 (C_{sp3}-H), 2238 (C≡N), 1776 (C=O), 1626 cm⁻¹ (C=C). HRMS (ESI⁺): *m/z* [M + H]⁺ calcd for C₉H₁₂NO₂ 166.0863; found 166.0894; [M + Na]⁺ calcd for C₉H₁₁NNaO₂ 188.0682; found 188.0698. Anal. Calcd for C₉H₁₁NO₂: C, 65.44; H, 6.71; N, 8.48. Found: C, 65.19; H, 6.50; N, 8.56.

3,3-Dimethyl-2-oxobutyl Cyanoacetate (1). Mp 46–51 °C. ¹H NMR (400 MHz, CDCl₃): δ = 4.99 (s, 2H), 3.60 (s, 2H), 1.20 ppm (s, 9H). ¹³C NMR (100 MHz, CDCl₃): δ = 206.3, 162.6, 112.7, 66.1, 42.7, 26.0, 24.3 ppm. IR (Nujol): $\bar{\nu}$ = 2261 (C≡N), 1759 (C=O), 1724 cm⁻¹ (C=O). HRMS (ESI⁺): *m/z* [M + Na]⁺ calcd for C₉H₁₃NNaO₃ 206.0788; found 206.0772. Anal. Calcd for C₉H₁₃NO₃: C, 59.00; H, 7.15; N, 7.65. Found: C, 58.75; H, 7.32; N, 7.85.

Compounds Py0(PhFu, Me₂Fu, BuFu). General Procedure. To a solution of aldehyde **Py0** (111 mg, 0.48 mmol) in absolute ethanol (5 mL) was added the corresponding acceptor (**PhFu**, **Me₂Fu**, **BuFu**) (0.48 mmol). (For the reaction with acceptor **Me₂Fu**, piperidine (one drop) was added.) The mixture was refluxed under argon with exclusion of light (TLC monitoring). In the case of **Py0PhFu** and **Py0Me₂Fu**, after cooling, the resulting solid was isolated by filtration, and washed with cold ethanol and a cold mixture of pentane/CH₂Cl₂ 9.5:0.5. In the case of **Py0BuFu**, the solvent was evaporated, and the crude product was purified by flash chromatography (silica gel).

(Z)-5-(2-(2,6-Di-tert-butyl-4H-pyran-4-ylidene)ethylidene)-2-oxo-4-phenyl-2,5-dihydrofuran-3-carbonitrile (PyOPhFu). Reaction time: 5 h. Evaporation of the filtrate and flash chromatography (silica gel) with CH₂Cl₂ as the eluent gave a second fraction. Yield: dark blue solid (118 mg; 62%). Mp 241–246 °C. ¹H NMR (400 MHz, CDCl₃): δ = 7.62–7.53 (m, 5H), 6.67 (d, J = 13.1 Hz, 1H), 6.18 (d, J = 1.8 Hz, 1H), 6.13 (d, J = 13.1 Hz, 1H), 6.07 (d, J = 1.8 Hz, 1H), 1.26 (s, 9H), 1.24 ppm (s, 9H). ¹³C NMR (100 MHz, CDCl₃): δ = 169.6, 169.3, 165.7, 157.6, 145.2, 141.3, 131.1, 129.2, 128.9, 120.8, 114.0, 113.7, 108.5, 107.5, 100.3, 91.1, 36.3, 36.1, 27.8 ppm. IR (Nujol): $\bar{\nu}$ = 2213 (C≡N), 1739 (C=O), 1655 (C=C), 1589 (C=C), 1567 cm⁻¹

(C=C). HRMS (ESI⁺): *m/z* [M + H]⁺ calcd for C₂₆H₂₈NO₃ 402.2064; found 402.2062; [M + Na]⁺ calcd for C₂₆H₂₇NNaO₃ 424.1883; found 424.1861; [2M + H]⁺ calcd for C₅₂H₅₅N₂O₆ 803.4055; found 803.4050; [2M + Na]⁺ calcd for C₅₂H₅₄N₂NaO₆ 825.3874; found 825.3862. Anal. Calcd for C₂₆H₂₇NO₃: C, 77.78; H, 6.78; N, 3.49. Found: C, 78.01; H, 6.54; N, 3.71.

(E)-4-(3-(2,6-Di-tert-butyl-4H-pyran-4-ylidene)prop-1-enyl)-5,5-dimethyl-2-oxo-2,5-dihydrofuran-3-carbonitrile (PyOMe₂Fu). Reaction time: 16 h 30 min. Evaporation of the filtrate and flash chromatography (silica gel) with CH₂Cl₂ as the eluent gave a second fraction. Yield: bright dark violet solid (122 mg; 69%). Mp 203–206 °C. ¹H NMR (400 MHz, CDCl₃): δ = 8.36 (dd, J₁ = 14.5 Hz, J₂ = 12.4 Hz, 1H), 6.47 (d, J = 1.9 Hz, 1H), 5.96 (d, J = 1.9 Hz, 1H), 5.79 (d, J = 14.5 Hz, 1H), 5.68 (d, J = 12.4 Hz, 1H), 1.52 (s, 6H), 1.28 (s, 9H), 1.25 ppm (s, 9H). ¹³C NMR (100 MHz, CDCl₃): δ = 176.4, 169.0, 168.9, 168.3, 145.6, 143.8, 115.6, 111.7, 108.9, 106.4, 100.7, 87.1, 86.0, 36.2, 36.0, 27.8, 26.0 ppm. IR (Nujol): $\bar{\nu}$ = 2206 (C≡N), 1738 (C=O), 1661 (C=C), 1596 (C=C), 1544 cm⁻¹ (C=C). HRMS (ESI⁺): *m/z* [M + H]⁺ calcd for C₂₃H₃₀NO₃ 368.2220; found 368.2196; [M + Na]⁺ calcd for C₂₃H₂₉NNaO₃ 390.2040; found 390.2012. Anal. Calcd for C₂₃H₂₉NO₃: C, 75.17; H, 7.95; N, 3.81. Found: C, 75.03; H, 8.13; N, 4.06.

(Z)-4-tert-butyl-5-(2-(2,6-di-tert-butyl-4H-pyran-4-ylidene)ethylidene)-2-oxo-2,5-dihydrofuran-3-carbonitrile (PyOBuFu). Reaction time: 5 h 30 min. Eluent chromatography: CH₂Cl₂/Et₂O 9.9:0.1. After column, the resulting solid was washed with a cold mixture of pentane/CH₂Cl₂ 9.5:0.5. Yield: dark violet solid (50 mg; 28%). Mp 226–229 °C. ¹H NMR (400 MHz, CDCl₃): δ = 6.98 (d, J = 12.6 Hz, 1H), 6.20 (d, J = 1.9 Hz, 1H), 6.04 (d, J = 12.6 Hz, 1H), 6.01 (d, J = 1.9 Hz, 1H), 1.55 (s, 9H), 1.28 (s, 9H), 1.25 ppm (s, 9H). ¹³C NMR (100 MHz, CDCl₃): δ = 168.9, 168.5, 167.7, 166.1, 143.7, 141.2, 120.7, 114.6, 107.8, 107.1, 99.7, 93.5, 36.2, 36.0, 35.1, 31.3, 27.8 ppm. IR (Nujol): $\bar{\nu}$ = 2215 (C≡N), 1746 (C=O), 1659 (C=C), 1588 (C=C), 1574 (C=C), 1512 cm⁻¹ (C=C); HRMS (ESI⁺): *m/z* [M + H]⁺ calcd for C₂₄H₃₂NO₃ 382.2377; found 382.2362; [M + Na]⁺ calcd for C₂₄H₃₁NNaO₃ 404.2196; found 404.2174; [M + K]⁺ calcd for C₂₄H₃₁KNO₃ 420.1936; found 420.1922. Anal. Calcd for C₂₄H₃₁NO₃: C, 75.56; H, 8.19; N, 3.67. Found: C, 75.34; H, 7.98; N, 3.83.

Compounds Py1(PhFu, Me₂Fu, BuFu). General Procedure. To a solution of aldehyde **Py1** (110 mg, 0.42 mmol) in absolute ethanol (5 mL) was added the corresponding acceptor (**PhFu**, **Me₂Fu**, **BuFu**) (0.42 mmol). (For the reaction with acceptor **Me₂Fu**, piperidine (one drop) was added.) The mixture was refluxed under argon with exclusion of light (TLC monitoring). After being cooled, the solvent was evaporated and the crude product was purified by flash chromatography (silica gel) with CH₂Cl₂ as the eluent. The resulting solid was washed with a cold mixture of pentane/CH₂Cl₂ 9.5:0.5.

(Z)-5-((E)-4-(2,6-Di-tert-butyl-4H-pyran-4-ylidene)but-2-enylidene)-2-oxo-4-phenyl-2,5-dihydrofuran-3-carbonitrile (Py1PhFu). Reaction time: 8 h 15 min. Yield: dark blue solid (43 mg; 24%). Mp 186–190 °C. ¹H NMR (400 MHz, CDCl₃): δ = 7.61–7.53 (m, 5H), 7.13 (dd, J₁ = 13.4 Hz, J₂ = 12.6 Hz, 1H), 6.65 (dd, J₁ = 13.4 Hz, J₂ = 12.2 Hz, 1H), 6.46 (dd, J₁ = 12.2 Hz, J₂ = 0.4 Hz, 1H), 6.24 (d, J = 1.8 Hz, 1H), 5.89 (d, J = 1.8 Hz, 1H), 5.73 (d, J = 12.6 Hz, 1H), 1.24 (s, 9H), 1.23 ppm (s, 9H). ¹³C NMR (100 MHz, CDCl₃): δ = 167.7, 167.6, 165.4, 158.1, 142.6, 142.4, 141.7, 131.2, 129.2, 128.9, 128.7, 125.9, 120.6, 114.0, 113.4, 106.5, 100.0, 92.6, 36.1, 35.9, 27.9, 27.8 ppm. IR (Nujol): $\bar{\nu}$ = 2217 (C≡N), 1742 (C=O), 1657 (C=C), 1557 (C=C), 1518 cm⁻¹ (C=C). HRMS (ESI⁺): *m/z* [M + H]⁺ calcd for C₂₈H₃₀NO₃ 428.2220; found 428.2209; [M + Na]⁺ calcd for C₂₈H₂₉NNaO₃ 450.2040; found 450.2011; [M + K]⁺ calcd for C₂₈H₂₉KNO₃ 466.1779; found 466.1748. Anal. Calcd for C₂₈H₂₉NO₃: C, 78.66; H, 6.84; N, 3.28. Found: C, 78.82; H, 6.74; N, 3.51.

4-((1E,3E)-5-(2,6-Di-tert-butyl-4H-pyran-4-ylidene)penta-1,3-dienyl)-5,5-dimethyl-2-oxo-2,5-dihydrofuran-3-carbonitrile (Py1-Me₂Fu). Reaction time: 9 h. Yield: dark green solid (33 mg; 20%). Mp 232–235 °C. ¹H NMR (400 MHz, CDCl₃): δ = 7.71 (dd, J₁ = 14.9 Hz, J₂ = 11.6 Hz, 1H), 7.19 (dd, J₁ = 13.8 Hz, J₂ = 12.5 Hz, 1H), 6.26 (d, J = 1.8 Hz, 1H), 6.22 (dd, J₁ = 13.8 Hz, J₂ = 11.6 Hz, 1H),

6.00 (d, $J = 14.9$ Hz, 1H), 5.83 (d, $J = 1.8$ Hz, 1H), 5.62 (d, $J = 12.5$ Hz, 1H), 1.56 (s, 6H), 1.27 (s, 9H), 1.22 ppm (s, 9H). ^{13}C NMR (100 MHz, CDCl_3): $\delta = 175.7, 167.8, 167.2, 166.8, 148.5, 142.4, 140.9, 125.1, 114.2, 112.6, 112.4, 106.0, 99.7, 90.3, 86.3, 36.1, 35.7, 27.9, 27.7, 26.1$ ppm. IR (Nujol): $\bar{\nu} = 2201$ ($\text{C}\equiv\text{N}$), 1742 ($\text{C}=\text{O}$), 1662 ($\text{C}=\text{C}$), 1576 cm^{-1} ($\text{C}=\text{C}$). HRMS (ESI^+): m/z [$\text{M} + \text{H}$] $^+$ calcd for $\text{C}_{25}\text{H}_{32}\text{NO}_3$ 394.2377; found 394.2378; calcd for [$\text{M} + \text{Na}$] $^+$ $\text{C}_{25}\text{H}_{31}\text{NNaO}_3$ 416.2196; found 416.2177. Anal. Calcd for $\text{C}_{25}\text{H}_{31}\text{NO}_3$: C, 76.30; H, 7.94; N, 3.56. Found: C, 76.45; H, 7.73; N, 3.83.

(*Z*)-4-*tert*-Butyl-5-((*E*)-4-(2-(2,6-di-*tert*-butyl-4*H*-pyran-4-ylidene)-but-2-enylidene)-2-oxo-2,5-dihydrofuran-3-carbonitrile) (**Py1BuFu**). Reaction time: 9 h. Yield: dark blue solid (39 mg; 23%). Mp 127–130 °C. ^1H NMR (400 MHz, CDCl_3): $\delta = 7.08$ (dd, $J_1 = 13.7$ Hz, $J_2 = 12.5$ Hz, 1H), 6.73 (d, $J = 11.9$ Hz, 1H), 6.59 (dd, $J_1 = 13.7$ Hz, $J_2 = 11.9$ Hz, 1H), 6.23 (d, $J = 1.6$ Hz, 1H), 5.84 (d, $J = 1.6$ Hz, 1H), 5.68 (d, $J = 12.5$ Hz, 1H), 1.54 (s, 9H), 1.26 (s, 9H), 1.22 ppm (s, 9H). ^{13}C NMR (100 MHz, CDCl_3): $\delta = 168.3, 167.0, 166.8, 165.7, 142.5, 140.9, 140.3, 125.7, 120.5, 114.2, 113.7, 106.2, 99.7, 95.1, 36.1, 35.8, 31.2, 29.7, 27.9, 27.8$ ppm. IR (Nujol): $\bar{\nu} = 2219$ ($\text{C}\equiv\text{N}$), 1749 ($\text{C}=\text{O}$), 1659 ($\text{C}=\text{C}$), 1558 cm^{-1} ($\text{C}=\text{C}$). HRMS (ESI^+): m/z [$\text{M} + \text{H}$] $^+$ calcd for $\text{C}_{26}\text{H}_{34}\text{NO}_3$ 408.2533; found 408.2514; [$\text{M} + \text{Na}$] $^+$ calcd for $\text{C}_{26}\text{H}_{33}\text{NNaO}_3$ 430.2353; found 430.2323; [$\text{M} + \text{K}$] $^+$ calcd for $\text{C}_{26}\text{H}_{33}\text{KNO}_3$ 446.2092; found 446.2055. Anal. Calcd for $\text{C}_{26}\text{H}_{33}\text{NO}_3$: C, 76.62; H, 8.16; N, 3.44. Found: C, 76.39; H, 8.45; N, 3.66.

Compounds Bz0(PhFu,Me₂Fu,BuFu). General Procedure. To a solution of benzothiazolium salt **Bz0** (60 mg; 0.15 mmol) and the corresponding acceptor (**PhFu,Me₂Fu,BuFu**) (0.15 mmol) in ethanol (1.6 mL) was added triethylamine (0.27 mL, 1.94 mmol). The mixture was refluxed under argon with exclusion of light (TLC monitoring). In the case of **Bz0PhFu**, after cooling, the resulting solid was isolated by filtration, and washed with cold ethanol and a cold mixture of pentane/ CH_2Cl_2 9.5:0.5. In the case of **Bz0Me₂Fu,Bz0BuFu**, the solvent was evaporated, and the crude product was purified by flash chromatography (silica gel).

(*Z*)-5-((*Z*)-2-(3-Ethylbenzothiazol-2(3*H*)-ylidene)ethylidene)-2-oxo-4-phenyl-2,5-dihydrofuran-3-carbonitrile (**Bz0PhFu**). Reaction time: 25 min. Yield: violet to grayish solid (32 mg; 59%). Mp 291–293 °C (ref 14, mp 279–281 °C). ^1H NMR (400 MHz, CDCl_3): $\delta = 7.63$ – 7.53 (m, 5H), 7.50 (dd, $J_1 = 7.9$ Hz, $J_2 = 1.0$ Hz, 1H), 7.42 (ddd, $J_1 = 8.4$ Hz, $J_2 = 7.6$ Hz, $J_3 = 1.0$ Hz, 1H), 7.23 (ddd, $J_1 = 7.9$ Hz, $J_2 = 7.6$ Hz, $J_3 = 0.9$ Hz, 1H), 7.17 (dd, $J_1 = 8.4$ Hz, $J_2 = 0.9$ Hz, 1H), 6.62 (d, $J = 12.6$ Hz, 1H), 6.22 (d, $J = 12.6$ Hz, 1H), 4.14 (q, $J = 7.3$ Hz, 2H), 1.44 ppm (t, $J = 7.3$ Hz, 3H). ^{13}C NMR (100 MHz, CDCl_3): $\delta = 166.7, 160.0, 155.4, 141.2, 138.3, 130.8, 129.4, 129.2, 128.9, 127.7, 124.7, 124.3, 123.8, 122.2, 114.5, 111.1, 104.7, 92.2, 41.0, 12.2$ ppm. IR (Nujol): $\bar{\nu} = 2207$ ($\text{C}\equiv\text{N}$), 1722 ($\text{C}=\text{O}$), 1691 ($\text{C}=\text{C}$), 1594 ($\text{C}=\text{C}$), 1576 ($\text{C}=\text{C}$), 1531 cm^{-1} ($\text{C}=\text{C}$). HRMS (ESI^+): m/z [$\text{M} + \text{H}$] $^+$ calcd for $\text{C}_{22}\text{H}_{17}\text{N}_2\text{O}_2\text{S}$ 373.1005; found 373.0988; [$\text{M} + \text{Na}$] $^+$ calcd for $\text{C}_{22}\text{H}_{16}\text{N}_2\text{NaO}_2\text{S}$ 395.0825; found 395.0803. Anal. Calcd for $\text{C}_{22}\text{H}_{16}\text{N}_2\text{O}_2\text{S}$: C, 70.95; H, 4.33; N, 7.52. Found: C, 71.04; H, 4.05; N, 7.58.

4-((1*E*,3*Z*)-3-(3-Ethylbenzothiazol-2(3*H*)-ylidene)prop-1-enyl)-5-dimethyl-2-oxo-2,5-dihydrofuran-3-carbonitrile (**Bz0Me₂Fu**). Reaction time: 35 min. Eluent chromatography: $\text{CH}_2\text{Cl}_2/\text{Et}_2\text{O}$ 9.6:0.4. Yield: dark violet solid (26 mg; 52%). Mp 248–251 °C. ^1H NMR (400 MHz, CD_3COCD_3): $\delta = 8.12$ (dd, $J_1 = 13.8$ Hz, $J_2 = 12.6$ Hz, 1H), 7.85 (ddd, $J_1 = 7.9$ Hz, $J_2 = 1.1$ Hz, $J_3 = 0.6$ Hz, 1H), 7.52–7.45 (m, 2H), 7.30 (ddd, $J_1 = 7.9$ Hz, $J_2 = 6.1$ Hz, $J_3 = 2.3$ Hz, 1H), 6.20 (d, $J = 12.6$ Hz, 1H), 5.97 (d, $J = 13.8$ Hz, 1H), 4.31 (q, $J = 7.2$ Hz, 2H), 1.53 (s, 6H), 1.41 ppm (t, $J = 7.2$ Hz, 3H). ^{13}C NMR (100 MHz, CD_3COCD_3): $\delta = 177.1, 170.0, 147.3, 143.4, 129.4, 126.8, 125.8, 124.4, 124.1, 118.1, 113.5, 106.6, 96.8, 87.1, 42.5, 27.7, 13.4$ ppm. IR (Nujol): $\bar{\nu} = 2210$ ($\text{C}\equiv\text{N}$), 1723 ($\text{C}=\text{O}$), 1581 ($\text{C}=\text{C}$), 1562 cm^{-1} ($\text{C}=\text{C}$). HRMS (ESI^+): m/z [$\text{M} + \text{H}$] $^+$ calcd for $\text{C}_{19}\text{H}_{19}\text{N}_2\text{O}_2\text{S}$ 339.1162; found 339.1136; [$\text{M} + \text{Na}$] $^+$ calcd for $\text{C}_{19}\text{H}_{18}\text{N}_2\text{NaO}_2\text{S}$ 361.0981; found 361.0945. Anal. Calcd for $\text{C}_{19}\text{H}_{18}\text{N}_2\text{O}_2\text{S}$: C, 67.43; H, 5.36; N, 8.28. Found: C, 67.65; H, 5.05; N, 8.49.

(*Z*)-5-((*Z*)-2-(3-Ethylbenzothiazol-2(3*H*)-ylidene)ethylidene)-2-oxo-4-*tert*-butyl-2,5-dihydrofuran-3-carbonitrile (**Bz0BuFu**). Reaction

time: 75 min. Eluent chromatography: $\text{CH}_2\text{Cl}_2/\text{Et}_2\text{O}$ 9.3:0.7. The solid obtained by flash chromatography was further washed with a mixture of pentane/ CH_2Cl_2 8.5/1.5. Yield: purple-violet solid (8 mg; 15%). Mp 265–268 °C. ^1H NMR (400 MHz, CD_2Cl_2): $\delta = 7.55$ (dd, $J_1 = 7.8$ Hz, $J_2 = 1.0$ Hz, 1H), 7.42 (ddd, $J_1 = 8.3$ Hz, $J_2 = 7.8$ Hz, $J_3 = 1.0$ Hz, 1H), 7.23 (td, $J_1 = 7.8$ Hz, $J_2 = 1.0$ Hz, 1H), 7.18 (d, $J = 8.3$ Hz, 1H), 7.03 (d, $J = 12.4$ Hz, 1H), 6.11 (d, $J = 12.4$ Hz, 1H), 4.13 (q, $J = 7.3$ Hz, 2H), 1.55 (s, 9H), 1.41 ppm (t, $J = 7.3$ Hz, 3H). ^{13}C NMR: not registered due to its low solubility. IR (Nujol): $\bar{\nu} = 2209$ ($\text{C}\equiv\text{N}$), 1720 ($\text{C}=\text{O}$), 1591 ($\text{C}=\text{C}$), 1531 cm^{-1} ($\text{C}=\text{C}$). HRMS (ESI^+): m/z [$\text{M} + \text{Na}$] $^+$ calcd for $\text{C}_{20}\text{H}_{20}\text{N}_2\text{NaO}_2\text{S}$ 375.1138; found 375.1140. Anal. Calcd for $\text{C}_{20}\text{H}_{20}\text{N}_2\text{O}_2\text{S}$: C, 68.16; H, 5.72; N, 7.95. Found: C, 68.34; H, 5.42; N, 7.80.

Compounds Bz1(PhFu,Me₂Fu,BuFu). General Procedure. To a solution of benzothiazolium salt **Bz1** (334 mg; 0.70 mmol) and the corresponding acceptor (**PhFu,Me₂Fu,BuFu**) (0.70 mmol) in ethanol (7.5 mL) was added triethylamine (1.3 mL, 9.32 mmol). The mixture was refluxed under argon with exclusion of light (TLC monitoring). After being cooled, the resulting solid was isolated by filtration, washed with cold ethanol and a cold mixture of pentane/ CH_2Cl_2 9.5/0.5, and finally purified by flash chromatography (silica gel) with $\text{CH}_2\text{Cl}_2/\text{Et}_2\text{O}$ 8:2 (9.2:0.8 for **Bz1Me₂Fu**) as the eluent.

(*Z*)-5-((2*E*,4*Z*)-4-(3-Ethylbenzothiazol-2(3*H*)-ylidene)but-2-enylidene)-2-oxo-4-phenyl-2,5-dihydrofuran-3-carbonitrile (**Bz1PhFu**). Reaction time: 25 min. The solid obtained by flash chromatography was further washed with a mixture of pentane/ CH_2Cl_2 7.5/2.5. Yield: Blue-green solid (81 mg; 29%). Mp 272–275 °C. ^1H NMR (400 MHz, CD_2Cl_2): 7.63–7.54 (m, 5H), 7.52 (d, $J = 7.8$ Hz, 1H), 7.39 (t, $J = 7.8$ Hz, 1H), 7.19 (t, $J = 7.8$ Hz, 1H), 7.16–7.07 (m, 2H), 6.64–6.53 (m, 2H), 5.96 (d, $J = 12.2$ Hz, 1H), 4.05 (q, $J = 7.2$ Hz, 2H), 1.39 ppm (t, $J = 7.2$ Hz, 3H). ^{13}C NMR: not registered due to its low solubility. IR (Nujol): $\bar{\nu} = 2200$ ($\text{C}\equiv\text{N}$), 1729 ($\text{C}=\text{O}$), 1556 cm^{-1} ($\text{C}=\text{C}$). HRMS (ESI^+): m/z [M] $^+$ calcd for $\text{C}_{24}\text{H}_{18}\text{N}_2\text{O}_2\text{S}$ 398.1083; found 398.1084; [$\text{M} + \text{Na}$] $^+$ calcd for $\text{C}_{24}\text{H}_{18}\text{N}_2\text{NaO}_2\text{S}$ 421.0981; found 421.0981. Anal. Calcd for $\text{C}_{24}\text{H}_{18}\text{N}_2\text{O}_2\text{S}$: C, 72.34; H, 4.55; N, 7.03. Found: C, 72.51; H, 4.34; N, 6.93.

4-((2*E*,4*Z*)-4-(3-Ethylbenzothiazol-2(3*H*)-ylidene)but-2-enylidene)-5,5-dimethyl-2-oxo-2,5-dihydrofuran-3-carbonitrile (**Bz1Me₂Fu**). Reaction time: 1 h. A further purification by flash chromatography on reverse C18 silica gel, with acetonitrile/aqueous $\text{CH}_3\text{COONH}_4$ 15 mM from 6:4 to 10:0, was needed. Yield: Deep blue solid (40 mg; 16%). Mp 254–259 °C. ^1H NMR (300 MHz, CD_2Cl_2): $\delta = 7.63$ (dd, $J_1 = 14.6$ Hz, $J_2 = 11.7$ Hz, 1H), 7.49 (dd, $J_1 = 7.7$ Hz, $J_2 = 1.0$ Hz, 1H), 7.34 (ddd, $J_1 = 8.2$ Hz, $J_2 = 7.7$ Hz, $J_3 = 1.0$ Hz, 1H), 7.14 (td, $J_1 = 7.7$ Hz, $J_2 = 1.0$ Hz, 1H), 7.11 (d, $J = 13.3$ Hz, 1H), 7.05 (d, $J = 8.2$ Hz, 1H), 6.22 (dd, $J_1 = 13.3$ Hz, $J_2 = 11.9$ Hz, 1H), 5.99 (d, $J = 14.6$ Hz, 1H), 5.78 (d, $J = 11.9$ Hz, 1H), 3.99 (q, $J = 7.2$ Hz, 2H), 1.56 (s, 6H), 1.36 ppm (t, $J = 7.2$ Hz, 3H). ^{13}C NMR: not registered due to its low solubility. IR (Nujol): $\bar{\nu} = 2213$ ($\text{C}\equiv\text{N}$), 1739 ($\text{C}=\text{O}$), 1651, 1581 cm^{-1} ($\text{C}=\text{C}$). HRMS (ESI^+): m/z [$\text{M} + \text{Na}$] $^+$ calcd for $\text{C}_{21}\text{H}_{20}\text{N}_2\text{NaO}_2\text{S}$ 387.1138; found 387.1144. Anal. Calcd for $\text{C}_{21}\text{H}_{20}\text{N}_2\text{O}_2\text{S}$: C, 69.21; H, 5.53; N, 7.69. Found: C, 69.10; H, 5.41; N, 7.80.

(*Z*)-4-*tert*-Butyl-5-((2*E*,4*Z*)-4-(3-ethylbenzothiazol-2(3*H*)-ylidene)but-2-enylidene)-2-oxo-2,5-dihydrofuran-3-carbonitrile (**Bz1BuFu**). Reaction time: 1 h. Yield: Blue-green solid (44 mg; 17%). Mp 241–245 °C. ^1H NMR (400 MHz, $\text{THF}-d_6$): $\delta = 7.51$ (dd, $J_1 = 7.8$ Hz, $J_2 = 1.2$ Hz, 1H), 7.31 (ddd, $J_1 = 8.2$ Hz, $J_2 = 7.4$ Hz, $J_3 = 1.2$ Hz, 1H), 7.19 (dd, $J_1 = 8.2$ Hz, $J_2 = 0.4$ Hz, 1H), 7.13–7.05 (m, 2H), 6.93 (dd, $J_1 = 11.8$ Hz, $J_2 = 0.6$ Hz, 1H), 6.52 (dd, $J_1 = 13.6$ Hz, $J_2 = 11.8$ Hz, 1H), 6.03 (d, $J = 11.8$ Hz, 1H), 4.08 (q, $J = 7.2$ Hz, 2H), 1.51 (s, 9H), 1.32 ppm (t, $J = 7.2$ Hz, 3H). ^{13}C NMR: not registered due to its low solubility. IR (Nujol): $\bar{\nu} = 2191$ ($\text{C}\equiv\text{N}$), 1702 ($\text{C}=\text{O}$), 1562 cm^{-1} ($\text{C}=\text{C}$). HRMS (ESI^+): m/z [M] $^+$ calcd for $\text{C}_{22}\text{H}_{22}\text{N}_2\text{O}_2\text{S}$ 378.1397; found 378.1393; [$\text{M} + \text{Na}$] $^+$ calcd for $\text{C}_{22}\text{H}_{22}\text{N}_2\text{NaO}_2\text{S}$ 401.1294; found 401.1299. Anal. Calcd for $\text{C}_{22}\text{H}_{22}\text{N}_2\text{O}_2\text{S}$: C, 69.81; H, 5.86; N, 7.40. Found: C, 70.10; H, 5.65; N, 7.56.

■ ASSOCIATED CONTENT

S Supporting Information

The Supporting Information is available free of charge on the ACS Publications website at DOI: 10.1021/acs.joc.5b02051.

General experimental methods, NMR and UV-vis spectra of new compounds, NLO measurements, X-ray crystallographic data and diagram of the crystal structures of **PyOPhFu**, **Py1PhFu**, **Py1Me₂Fu**, and **BzOPhFu**, IR-spectroelectrochemistry studies, computed energies and Cartesian coordinates of optimized geometries, and contour plots of frontier molecular orbitals of all chromophores with the exception of **Py1BuFu** (PDF)

X-ray data for compound **BzOPhFu** (CIF)

X-ray data for compound **PyOPhFu** (CIF)

X-ray data for compound **Py1PhFu** (CIF)

X-ray data for compound **Py1Me₂Fu** (CIF)

■ AUTHOR INFORMATION

Corresponding Authors

*E-mail: casado@uma.es.

*E-mail: randreu@unizar.es.

Notes

The authors declare no competing financial interest.

■ ACKNOWLEDGMENTS

We thank Dr. E. Galán (Delft University of Technology, The Netherlands) for helpful discussions. Financial support from MICINN-FEDER (CTQ2011-22727 and MAT2011-27978-C02-02), MINECO (CTQ2014-52331R), and Gobierno de Aragón-Fondo Social Europeo (E39 and E04) is gratefully acknowledged. Research at the Universidad de Málaga was supported by MINECO (CTQ2012-33733) and Junta de Andalucía (P09-4708). We would like to acknowledge the use of Servicio General de Apoyo a la Investigación-SAI, Universidad de Zaragoza.

■ REFERENCES

- (1) (a) Themed issue on organic nonlinear optics: Marder, S. R., Guest Ed. *J. Mater. Chem.* **2009**, *19*. (b) Dalton, L. R.; Sullivan, P. A.; Bale, D. H. *Chem. Rev.* **2010**, *110*, 25–55. (c) Stegeman, G. I.; Stegeman, R. A. In *Nonlinear Optics: Phenomena, Materials, and Devices*; Boreman, G., Ed.; Wiley Series in Pure and Applied Optics; John Wiley & Sons: Hoboken, 2012. (d) Coe, B. J. *Coord. Chem. Rev.* **2013**, *257*, 1438–1458. (e) Castet, F.; Rodriguez, V.; Pozzo, J.-L.; Ducasse, L.; Plaquet, A.; Champagne, B. *Acc. Chem. Res.* **2013**, *46*, 2656–2665.
- (2) Bureš, F. *RSC Adv.* **2014**, *4*, 58826–58851 and references cited therein.
- (3) (a) Marder, S. R.; Perry, J. W.; Tiemann, B. G.; Gorman, C. B.; Gilmour, S.; Biddle, S. L.; Bourhill, G. *J. Am. Chem. Soc.* **1993**, *115*, 2524–2526. (b) Bourhill, G.; Brédas, J.-L.; Cheng, L.-T.; Marder, S. R.; Meyers, F.; Perry, J. W.; Tiemann, B. G. *J. Am. Chem. Soc.* **1994**, *116*, 2619–2620.
- (4) (a) Marder, S. R.; Beratan, D. N.; Cheng, L.-T. *Science* **1991**, *252*, 103–106. (b) Gorman, C. B.; Marder, S. R. *Proc. Natl. Acad. Sci. U. S. A.* **1993**, *90*, 11297–11301. (c) Meyers, F.; Marder, S. R.; Pierce, B. M.; Brédas, J.-L. *J. Am. Chem. Soc.* **1994**, *116*, 10703–10714. (d) Marder, S. R.; Gorman, C. B.; Meyers, F.; Perry, J. W.; Bourhill, G.; Brédas, J.-L.; Pierce, B. M. *Science* **1994**, *265*, 632–635.
- (5) (a) Stiegman, A. E.; Graham, E.; Perry, K. J.; Khundkar, L. R.; Cheng, L.-T.; Perry, J. W. *J. Am. Chem. Soc.* **1991**, *113*, 7658–7666. (b) Cheng, L.-T.; Tam, W.; Marder, S. R.; Stiegman, A. E.; Rikken, G.; Spangler, C. W. *J. Phys. Chem.* **1991**, *95*, 10643–10652. (c) de Lucas, A. I.; Martín, N.; Sánchez, L.; Seoane, C.; Andreu, R.; Garín, J.;

Orduna, J.; Alcalá, R.; Villacampa, B. *Tetrahedron* **1998**, *54*, 4655–4662. (d) Moreno-Mañas, M.; Pleixats, R.; Andreu, R.; Garín, J.; Orduna, J.; Villacampa, B.; Levillain, E.; Sallé, M. *J. Mater. Chem.* **2001**, *11*, 374–380. (e) González, M.; Segura, J. L.; Seoane, C.; Martín, N.; Garín, J.; Orduna, J.; Alcalá, R.; Villacampa, B.; Hernández, V.; López Navarrete, J. T. *J. Org. Chem.* **2001**, *66*, 8872–8882.

(6) The term “butenolide” for describing buteno- or crotonolactones was first employed by Klobb in 1898: Klobb, T. *Bull. Soc. Chim. Fr.* **1898**, 389. Although the butenolide nomenclature has been in vogue for quite sometime, *Chemical Abstracts* currently has adopted the furanone system for naming these compounds. Thus, $\Delta^{\alpha,\beta}$ -butenolides are 2(*SH*)-furanones. In this Article, the terms butenolide/furanone will be used interchangeably.

(7) (a) Rao, Y. S. *Chem. Rev.* **1976**, *76*, 625–694. (b) Carter, N. B.; Nadany, A. E.; Sweeny, J. B. *J. Chem. Soc., Perkin Trans. 1* **2002**, 2324–2342. (c) Ugurchieva, T. M.; Veselovsky, V. V. *Russ. Chem. Rev.* **2009**, *78*, 337–373.

(8) (a) Wang, P.; Chang, Y.; Xu, Y.; Ye, C. *Proc. SPIE* **1998**, *3556*, 73–83. (b) Asthana, D.; Ajayakumar, M. R.; Pant, R. P.; Mukhopadhyay, P. *Chem. Commun.* **2012**, *48*, 6475–6477.

(9) (a) Zhang, C.; Dalton, L. R.; Oh, M.-C.; Zhang, H.; Steier, W. H. *Chem. Mater.* **2001**, *13*, 3043–3050. (b) Liao, Y.; Eichinger, B. E.; Firestone, K. A.; Haller, M.; Luo, J.; Kaminsky, W.; Benedict, J. B.; Reid, P. J.; Jen, A. K.-Y.; Dalton, L. R.; Robinson, B. H. *J. Am. Chem. Soc.* **2005**, *127*, 2758–2766.

(10) Selected examples for 4*H*-pyranylidene-containing chromophores: (a) Faux, N.; Caro, B.; Robin-le Guen, F.; Le Poul, P.; Nakatani, K.; Ishow, E. *J. Organomet. Chem.* **2005**, *690*, 4982–4988. (b) Andreu, R.; Carrasquer, L.; Franco, S.; Garín, J.; Orduna, J.; Martínez de Baroja, N.; Alicante, R.; Villacampa, B.; Allain, M. *J. Org. Chem.* **2009**, *74*, 6647–6657. (c) Andreu, R.; Galán, E.; Orduna, J.; Villacampa, B.; Alicante, R.; López Navarrete, J. T.; Casado, J.; Garín, J. *Chem. - Eur. J.* **2011**, *17*, 826–838. (d) Achelle, S.; Malval, J.-P.; Aloïse, S.; Barsella, A.; Spangenberg, A.; Mager, L.; Akdas-Kilig, H.; Fillaut, J.-L.; Caro, B.; Robin-le Guen, F. *ChemPhysChem* **2013**, *14*, 2725–2736. (e) Marco, A. B.; Martínez de Baroja, N.; Franco, S.; Garín, J.; Orduna, J.; Villacampa, B.; Revuelto, A.; Andreu, R. *Chem. - Asian J.* **2015**, *10*, 188–197.

(11) Selected examples: (a) Ashwell, G. J.; Malhotra, M.; Bryce, M. R.; Grainger, A. M. *Synth. Met.* **1991**, *41–43*, 3173–3176. (b) Kay, A. J.; Woolhouse, A. D.; Gainsford, G. J.; Haskell, T. G.; Barnes, T. H.; McKinnie, I. T.; Wyss, C. P. *J. Mater. Chem.* **2001**, *11*, 996–1002. (c) Kay, A. J.; Woolhouse, A. D.; Zhao, Y.; Clays, K. *J. Mater. Chem.* **2004**, *14*, 1321–1330. (d) Latorre, S.; Moreira, I. de P. R.; Villacampa, B.; Julià, L.; Velasco, D.; Bofill, J. M.; López-Calahorra, F. *ChemPhysChem* **2010**, *11*, 912–919. (e) Andreu, R.; Galán, E.; Garín, J.; Orduna, J.; Alicante, R.; Villacampa, B. *Tetrahedron Lett.* **2010**, *51*, 6863–6866.

(12) Selected examples: (a) Coe, B. J.; Harris, J. A.; Hall, J. J.; Brunschwig, B. S.; Hung, S.-T.; Libaers, W.; Clays, K.; Coles, S. J.; Horton, P. N.; Light, M. E.; Hursthouse, M. B.; Garín, J.; Orduna, J. *Chem. Mater.* **2006**, *18*, 5907–5918. (b) Hrobárik, P.; Sigmundová, I.; Zahradník, P.; Kasák, P.; Arion, V.; Franz, E.; Clays, K. *J. Phys. Chem. C* **2010**, *114*, 22289–22302. (c) Hrobárik, P.; Hrobáriková, V.; Sigmundová, I.; Zahradník, P.; Fakis, M.; Polyzos, I.; Persephonis, P. *J. Org. Chem.* **2011**, *76*, 8726–8736. (d) Raposo, M. M. M.; Castro, M. C. R.; Belsley, M.; Fonseca, A. M. C. *Dyes Pigm.* **2011**, *91*, 454–465.

(13) Hrobárik, P.; Zahradník, P.; Fabian, W. M. F. *Phys. Chem. Chem. Phys.* **2004**, *6*, 495–502.

(14) Acceptor **PhFu**: Ford, J. A., Jr.; Wilson, C. V.; Young, W. R. *J. Org. Chem.* **1967**, *32*, 173–177.

(15) Acceptor **Me₂Fu**: (a) Cheikh, N.; Villemin, D.; Bar, N.; Lohier, J.-F.; Choukchou-Braham, N.; Mostefa-Kara, B.; Sopkova, J. *Tetrahedron* **2013**, *69*, 1234–1247. (b) For this work, acceptor **Me₂Fu** was prepared by following the same procedure reported for the corresponding analogue with methyl and ethyl groups in **C5**: Maheut, G.; Liao, L.; Catel, J.-M.; Jaffrès, P.-A.; Villemin, D. *J. Chem. Educ.* **2001**, *78*, 654–657.

- (16) Acceptor **BuFu**: Erdmann, D.; Schuehrer, K.; Koch, W.; Schneider, G. Patent DE 2116416, 1972; *Chem. Abstr.* **1973**, *78*, 16015.
- (17) Andreu, R.; Galán, E.; Garín, J.; Herrero, V.; Lacarra, E.; Orduna, J.; Alicante, R.; Villacampa, B. *J. Org. Chem.* **2010**, *75*, 1684–1692.
- (18) See, for example: (a) Alías, S.; Andreu, R.; Blesa, M. J.; Cerdán, M. A.; Franco, S.; Garín, J.; López, C.; Orduna, J.; Sanz, J.; Alicante, R.; Villacampa, B.; Allain, M. *J. Org. Chem.* **2008**, *73*, 5890–5898. (b) Marco, A. B.; Andreu, R.; Franco, S.; Garín, J.; Orduna, J.; Villacampa, B.; Alicante, R. *Tetrahedron* **2013**, *69*, 3919–3926.
- (19) (a) Coe, B. J.; Harris, J. A.; Asselberghs, I.; Wostyn, K.; Clays, K.; Persoons, A.; Brunshwing, B. S.; Coles, S. J.; Gelbrich, T.; Light, M. E.; Hursthouse, M. B.; Nakatani, K. *Adv. Funct. Mater.* **2003**, *13*, 347–357. (b) Beverina, L.; Fu, J.; Leclercq, A.; Zojer, E.; Pacher, P.; Barlow, S.; van Stryland, E. W.; Hagan, D. J.; Brédas, J.-L.; Marder, S. R. *J. Am. Chem. Soc.* **2005**, *127*, 7282–7283.
- (20) Brooker, L. G. S.; White, F. L.; Keyes, G. H.; Smyth, C. P.; Oesper, P. F. *J. Am. Chem. Soc.* **1941**, *63*, 3192–3203.
- (21) (a) Dehu, C.; Meyers, F.; Brédas, J.-L. *J. Am. Chem. Soc.* **1993**, *115*, 6198–6206. (b) Hilger, A.; Gisselbrecht, J.-P.; Tykewski, R. R.; Boudon, C.; Schreiber, M.; Martin, R. E.; Lüthi, H. P.; Gross, M.; Diederich, F. *J. Am. Chem. Soc.* **1997**, *119*, 2069–2078.
- (22) Bird, C. W. *Tetrahedron* **1986**, *42*, 89–92.
- (23) Marco, A. B.; Mayorga Burrezo, P.; Mosteo, L.; Franco, S.; Garín, J.; Orduna, J.; Diosdado, B. E.; Villacampa, B.; López Navarrete, J. T.; Casado, J.; Andreu, R. *RSC Adv.* **2015**, *5*, 231–242.
- (24) Chasseau, D.; Gaultier, J.; Hauw, C.; Fugnitto, R.; Gianis, V.; Strzelecka, H. *Acta Crystallogr., Sect. B: Struct. Crystallogr. Cryst. Chem.* **1982**, *38*, 1629–1631.
- (25) Marder, S. R.; Cheng, L.-T.; Tiemann, B. G.; Friedli, A. C.; Blanchard-Desce, M.; Perry, J. W.; Skindhøj, J. *Science* **1994**, *263*, 511–514.
- (26) Chang, Y. M. *Huaxue Tongbao* **1996**, *10*, 58–60.
- (27) Poronik, Y. M.; Hugues, V.; Blanchard-Desce, M.; Gryko, D. T. *Chem. - Eur. J.* **2012**, *18*, 9258–9266.
- (28) (a) Marder, S. R.; Perry, J. W.; Bourhill, G.; Gorman, C. B.; Tiemann, B. G.; Mansour, K. *Science* **1993**, *261*, 186–189. (b) For all-trans polyenes $\Delta J \approx 6.0$ Hz and for cyanines $\Delta J = 0$ Hz: Scheibe, G.; Seiffert, W.; Hohlneicher, G.; Jutz, C.; Springer, H. J. *Tetrahedron Lett.* **1966**, *7*, 5053–5059.
- (29) Kulinich, A. V.; Ishchenko, A. A.; Groth, U. M. *Spectrochim. Acta, Part A* **2007**, *68*, 6–14.
- (30) (a) Brooker, L. G. S.; Sklar, A. L.; Creesman, H. W. J.; Keyes, G. H.; Smith, L. A.; Sprague, R. H.; Van Lare, E.; Van Zandt, G.; White, F. L.; Williams, W. W. *J. Am. Chem. Soc.* **1945**, *67*, 1875–1889. (b) Bricks, J. L.; Kachkovskii, A. D.; Slominskii, Yu. L.; Gerasov, A. O.; Popov, S. V. *Dyes Pigm.* **2015**, *121*, 238–255.
- (31) Casado, J.; Moreno Oliva, M.; Ruiz Delgado, M. C.; López Navarrete, J. T.; Sánchez, L.; Martín, N.; Andreu, R.; Carrasquer, L.; Garín, J.; Orduna, J. *J. Chem. Phys.* **2007**, *126*, 074701–1–074701–8.
- (32) (a) Inoue, S.; Aso, Y.; Otsubo, T. *Chem. Commun.* **1997**, 1105–1106. (b) Milián, B.; Ortí, E.; Hernández, V.; López Navarrete, J. T.; Otsubo, T. *J. Phys. Chem. B* **2003**, *107*, 12175–12183. (c) Kang, H.; Facchetti, A.; Jiang, H.; Cariati, E.; Righetto, S.; Ugo, R.; Zuccaccia, C.; Macchioni, A.; Stern, C. L.; Liu, Z.; Ho, S.-T.; Brown, E. C.; Ratner, M. A.; Marks, T. J. *J. Am. Chem. Soc.* **2007**, *129*, 3267–3286.
- (33) This effect is well known as “vinylene shift”; see, for example: Kachkovskii, A. D.; Kovalenko, N. M. *Dyes Pigm.* **1997**, *35*, 131–148.
- (34) Kurdyukov, V. V.; Ishchenko, A. A.; Kudinova, M. A.; Tolmachev, A. I. *Chem. Heterocycl. Compd.* **1987**, *23*, 628–633.
- (35) Ikeda, H.; Sakai, T.; Kawasaki, K. *Chem. Phys. Lett.* **1991**, *179*, 551–554.
- (36) This behavior has already been reported for other D- π -A systems: (a) Reference 23. (b) Kim, O.-K.; Fort, A.; Barzoukas, M.; Blanchard-Desce, M.; Lehn, J.-M. *J. Mater. Chem.* **1999**, *9*, 2227–2232. (c) Davies, J. A.; Elangovan, A.; Sullivan, P. A.; Olbricht, B. C.; Bale, D. H.; Ewy, T. R.; Isborn, C. M.; Eichinger, B. E.; Robinson, B. H.; Reid, P. J.; Li, X.; Dalton, L. R. *J. Am. Chem. Soc.* **2008**, *130*, 10565–10575.
- (d) Marco, A. B.; Andreu, R.; Franco, S.; Garín, J.; Orduna, J.; Villacampa, B.; Diosdado, B. E.; López Navarrete, J. T.; Casado, J. *Org. Biomol. Chem.* **2013**, *11*, 6338–6349.
- (37) (a) Oudar, J. L.; Chemla, D. S. *J. Chem. Phys.* **1977**, *66*, 2664–2668. (b) Kanis, D. R.; Ratner, M. A.; Marks, T. J. *Chem. Rev.* **1994**, *94*, 195–242.
- (38) Faux, N.; Robin-le Guen, F.; Le Poul, P.; Caro, B.; Nakatani, K.; Ishow, E.; Golhen, S. *Eur. J. Inorg. Chem.* **2006**, 3489–3497.
- (39) Cho, B. R.; Je, J. T.; Lee, S. J.; Lee, S. H.; Kim, H. S.; Jeon, S. J.; Song, O.-K.; Wang, C. H. *J. Chem. Soc., Perkin Trans. 2* **1996**, 2141–2144.